Global Water Cycle: Extension Across the Earth Sciences

Progress Report
NASA Earth Observing System
NAGW-2686
January 1997

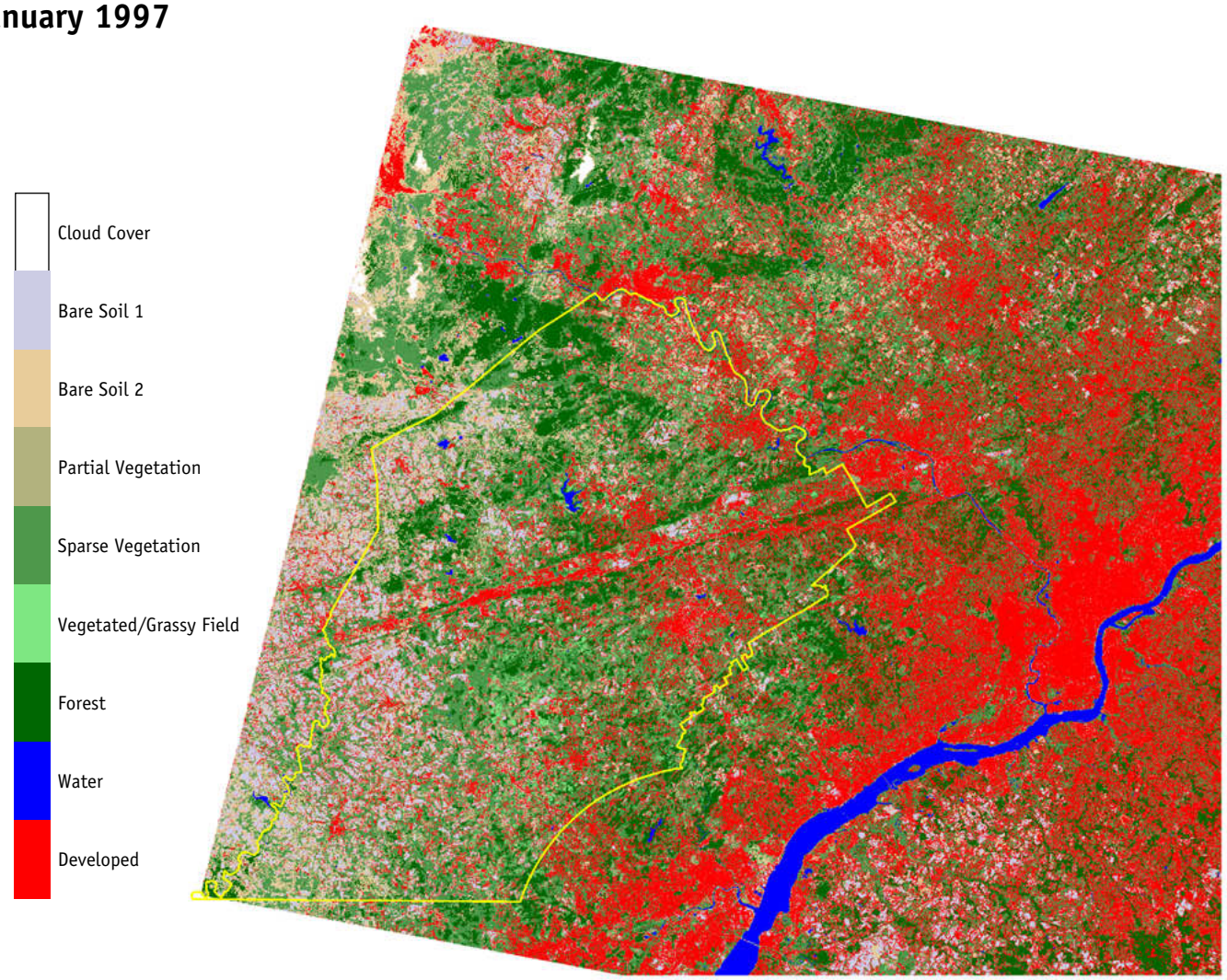

Classified Landsat TM image for June 2, 1996 over Chester County, PA

Principal Investigators

Eric J. Barron
Franklin Robertson
Tom Ackerman
Richard Alley
Bruce Albrecht
Toby Carlson
John Christy
Robert Crane
Steve Goodman
Lee Kump
Art Miller
Timothy Miller
Gary Petersen
Donna Peuquet
Rudy Slingerland
Brent Yarnal

Contributing Scientists

Dan Fitzjarrald
Rob Gillies
Greg Jenkins
Mercedes Lakhtakia
Dennis Lamb
Doug Miller
Richard White

PENNSTATE
1855
Earth System Science Center

NASA
National Aeronautics and Space Administration
George C. Marshall Space Flight Center

Abstract

Despite the significance of water, our knowledge of it as part of the global, interacting system is meager. Consequently, we are far from understanding how the hydrologic cycle will respond to a changing Earth system, or the nature of water's influence across the components of the system. To address these issues, the primary research strategy of this investigation, centers on nesting or coupling coarse resolution GCMs, with high resolution mesoscale models, with models including soil moisture, vegetation, and surface and groundwater hydrology. In this manner, we are attempting to produce global change predictions, in response to a variety of factors ranging from increases in greenhouse gas concentrations to changes in land cover, at a spatial scale which is appropriate to assess their impact. This research strategy is accomplished through an emphasis on integrated regional studies and the development of coupled earth system models. A basic requirement to accomplish these goals is also to develop data sets for initialization and validation of the various models at a variety of spatial scales, and to focus on critical limitations in current models (e.g. cloud parameterizations). During this process, we also contribute to the production of data sets which describe changes in climate and the nature of climate variability.

Background

The critical facets of climate and hydrology research needs have been described in NRC reports (e.g. 1985), in planning documents of the USGCRP and the WCRP (e.g. CLIVAR and GEWEX), and in Earth System Science: A program for global change. The primary research objectives are clear: determine and understand the dynamics of the major reservoirs of water, the mechanisms for transfers of water between global reservoirs, predict changes in the distributions, volumes, fluxes of water resulting from change and from human activities, and understand better the coupling of water with other components of the Earth system. We are developing methodologies and modeling capabilities to describe quantitatively the presently uncertain rates associated with the sources, sinks, and fluxes of the global water cycle with the ultimate goal of increasing our ability to predict changes in the hydrologic cycle associated with natural variability and human activities. A key element is to address changes in the hydrologic cycle at a scale appropriate for considering its impact on human activities, including agriculture and water resources. The proposed research included 31 specific objectives, which are summarized here, for the sake of brevity, as 9 primary objectives:

1. Evaluate GCM capability to simulate hydrologic cycle components
2. Evaluate GCM sensitivity to lower boundary forcing
3. Generate global data sets for documentation of global change, specifically for hydrologic variables, and for global model validation and verification
4. Develop improved treatment of cloud and precipitation processes
5. Develop and test components of high resolution regional atmospheric models critical for water and energy fluxes
6. Test the adaptability of terrestrial hydrologic models for sensitivity to spatial and topographic scales
7. Develop and test indirect measures of soil water content, with the objective of integrating these results into mesoscale model simulations
8. Develop and test coupled (nested) GCM-Mesoscale-Hydrologic Forecast models
9. Develop comprehensive databases and GIS for regions, such as the Susquehanna River Basin, the Cape Region, and others, to facilitate the development and evaluation of the nested model approach to regional prediction

These objectives incorporate three major integrating elements: (1) Documentation of Earth system change (4-dimensional multiphase water, temperature and diabatic heating, ice sheet mass balance, and regional scale terrestrial and atmospheric water and energy budgets), (2) Focused studies on controlling processes (cloud processes, the interface of the atmosphere with ocean, cryosphere, biosphere and land surface), and (3) Integrated conceptual and predictive models (extension of predictive capability across a spectrum of spatial scales, verification and validation of hydrologic cycle predictive capability, and coupled Earth system models).

The objectives and the integrating elements include a large number of challenging scientific issues requiring focused research and the interactions of a significant number of disciplines. Such a comprehensive set of objectives presents challenges for even a large team of investigators. As a practical element, the significant advances of this project are occurring because of the development of regional-scale experiments; designed to improve understanding of important physical processes, develop coupled models, and assess and validate model predictions. Almost the entire

research team contributes to these regional-scale experiments, each cooperatively seeking to advance the research objectives outlined above.

To date, much of the emphasis of the project has focused on the Susquehanna River Basin, with additional research on the Cape region of Florida. Much of the future work is proposed for the Ohio and Tennessee River Basins. These regions have been the focal point for assessing GCM capability, coupling and evaluating GCMs with mesoscale models, incorporating improved surface processes within the mesoscale models, integrating soil moisture measurements and models, evaluating and linking terrestrial hydrologic models of surface flow and groundwater, developing comprehensive GIS with a full spectrum of data for specification of model boundary conditions and evaluating predictions, and linking these models with other elements of the Earth system (e.g. landscape evolution) and societally-important issues (e.g. impacts of changes in the hydrologic cycle on agriculture).

The primary research strategy of this investigation, therefore, centers on nesting or coupling coarse resolution GCMs, with high resolution mesoscale models, with models including soil moisture, vegetation, and surface and groundwater hydrology. In this manner, we are attempting to produce global change predictions, in response to a variety of factors ranging from increases in greenhouse gas concentrations to changes in land cover, at a spatial scale which is appropriate to assess their impact. Such a strategy introduces the potential that we will link the errors of one model with the errors of each of the nested models. However, we have not jumped to make regional global change predictions. Rather, our efforts are directed to a series of careful studies designed to improve understanding and assess model capability critically. The completed and planned studies of this investigation are not only describing the uncertainties, but are, perhaps more importantly, substantially increasing our knowledge of a variety of processes, and providing a strong foundation for high resolution, coupled Earth system models. We are establishing a greater capability to utilize EOS observations to describe key hydrologic and climatic processes, to further develop and validate models, increasing our understanding of the past and the future and their relationships to Earth system components and thus providing a more robust predictive capability.

Data Sets for Documentation of Global Change

Evaluation Of Longwave Clear-Sky Data Sets

(F. Robertson and D. Fitzjarrald—MSFC)

The fundamental role of water vapor in linking radiation, convection and dynamics has been widely studied and debated as a classical problem in climate dynamics. Water vapor feedback associated with climate change has been a subject of particular controversy since it is judged to be the principal mechanism supporting claims of global warming scenarios.

Two years ago we began validating GENESIS AMIP-type simulations with ERBS data. In particular we investigated the change in longwave clear-sky radiation (LWCS) during the period 1985–1989 (Figure 1). This particular diagnostic is a crucial measure of the linkage between radiation, deep convection, and atmospheric dynamics. Our motivation in part was that any credible climate variability simulation linking global and regional models would have to replicate convective processes that give rise to these radiative signatures. This year we have spent considerable time in understanding the ERBS measurements in comparison to two other independent LWCS estimates. One produced at University of Maryland (UMD) is a statistical algorithm using four HIRS2 channels; the other is from the GSFC TOVS Path A Pathfinder data set. Our major findings are summarized as follows:

1. ERBS, TOVS Path A, and UMD clear-sky TOA fluxes each capture an areally-integrated signal of interannual variability associated with the '87–'88 El Nino / La Nina. Potential problems associated with cloud identification and clearing may be non-negligible, but do not change the conclusion that averaged over the tropical oceans there is a clear modulation of LWCS by water vapor during the 1987/1989 period.

2. ERBS mistakenly classifies many clear but moist atmospheres as being cloudy. Consequently, the amplitude of water vapor forcing effects on LWCS variability is underestimated. The UMD LWCS product, which is totally independent of ERBS, has a high degree of correlation with ERBS but interannual LWCS anomalies are of larger amplitude.

3. After accounting for ERBS problems we find that during the 1987/88 ENSO event there is an increase in water vapor trapping of LWCS as tropical mean SSTs increase. Were it not for this effect the tropical ocean areas would tend to equilibrate by rejecting additional energy at the rate of 6.0 W/m/m/K. However the effect of the additional water vapor is to reduce this rate of relaxation toward normal conditions to approximately 3.0 W/m/m/K. These measurements contain valuable information on how interannual anomalies in tropical heat balance are equilibrated.

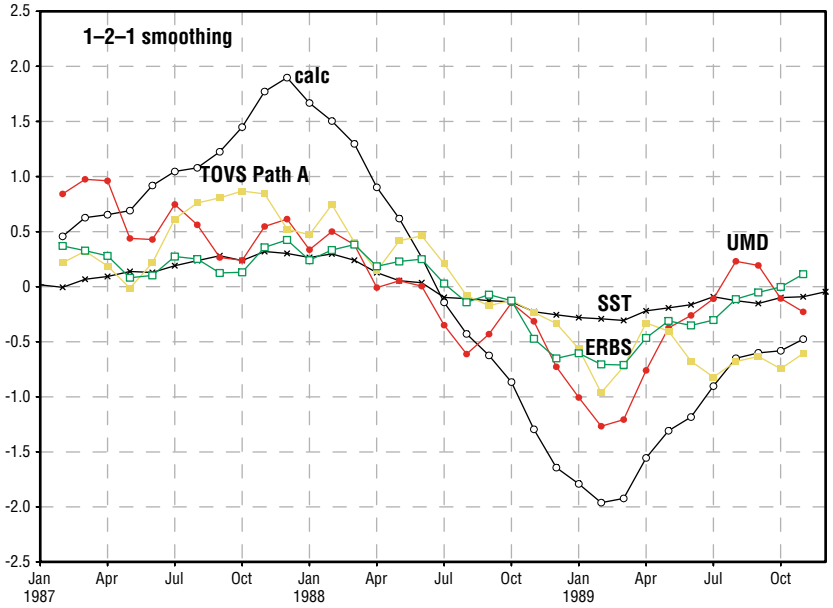

Figure 1. Monthly mean anomalies (W/m^2) in top-of-atmosphere longwave clear-sky radiation (LCWS) averaged over the tropical oceans (30 degrees N, S). Also shown are corresponding SST anomalies and a radiative transfer calculation of LWCS that would have occurred with SST and atmospheric temperature pertubations, but no variation in water vapor. Anomalies are departure from annual cycle defined by 1987/1989

These findings are subject to the caveat that the tropical oceanic region is not energetically closed, but exchanges moisture, heat, and mass with higher latitudes and with the tropical land areas. Thus our findings can not yet be strictly interpreted as a measure of water vapor feedback. In attempting to evaluate these boundary transports, we have found a significant difference between NCEP and GSFC/DAO diagnostics of moisture and energy flux anomalies into and out of the tropical ocean regions. Bringing to bear the resources of EOS observations to reduce these uncertainties is an important problem for the NASA climate community. We are currently addressing some aspects of this problem.

During FY97 we anticipate two main extensions of this effort. The first of these is to extend these diagnostics using the UMD LWCS product for the period covered by NOAA 12. This will enable comparison to similar diagnostics done for the 1993–1995 period using a microwave algorithm developed by Dr. Roy Spencer. We also are now confident that this diagnostic calculation we have made can be used to validate global climate model simulations of ENSO events and the changes that water vapor makes in LWCS. These products will feed into validation of regional climate variability simulations.

An Integrated Moisture And Heat Budget Analysis

(F. Robertson and D. Fitzjarrald, E.W. McCaul, H.-I. Lu—MSFC)

In previous work to construct large-scale moisture budgets we relied upon vertical motion fields from reanalysis centers (e.g. DAO, ECMWF, and NMC) to drive transport models of parameterized microphysical cloud processes. It soon became obvious that the accuracy of the vertical motion fields and associated divergence were less than adequate. Specifically there were many inconsistencies of vertical motion with pre-EOS measurements of precipitation, water vapor, and radiation. We have defined a strategy for producing revised kinematic fields which satisfy energy and water balance and the diabatic forcing retrieved from pre-EOS measurements.

Our strategy is a simple variational approach which enforces as integral constraints such data as GPCP precipitation, SRB net radiation at the surface, ERBS TOA net radiation, and ocean surface latent and sensible heat fluxes from SSM/I. Starting with a first guess vertical motion field the variational constraints are modified so that both the heat and water vapor balance equations reproduce the observed forcing. This method is adept at recovering horizontal structure, but as yet, only modifies two modes in the vertical. The vertical structure modifications to the divergent circulation are crucial however since these imbalances in current analyses give rise to errors when examining such processes as interannual variability in ENSO or monsoon strength. We have examined the error characteristics of the constraining data sets relative to existing reanalysis fields to insure that they can contribute new information. For example, Figure 2 shows the vertically-integrated atmospheric radiative cooling synthesized from SRB and ERBS observations compared to the DAO assimilated result. Significant differences (which consequently affect the vertical moon fields) are noted.

We are currently implementing the variational procedure and will use it to produce monthly mean omega and divergence fields along with heat and moisture balance diagnostics, which will be compared to results from the recent upgraded GEOS assimilation. This will most likely involve the TOGA COARE period.

The science requirements for this type of data set are broad and cover many interdisciplinary topics identified by MTPE and EOS. Researchers involved in diagnostics of climate variability on interannual time scales need accurate divergent circulation data. Examples of these studies include tropical forcing of middle latitudes, heat and water budget diagnostics, circulation anomalies over the GCIP, LBA, and other GEWEX hydrometeorology regional experiments, and pollutant

or constituent transport and dispersal related to biomass burning. Global climate modelers will have a data set for validation of the divergent circulation that has a degree of internal consistency and observational constraint that is nonexistent today.

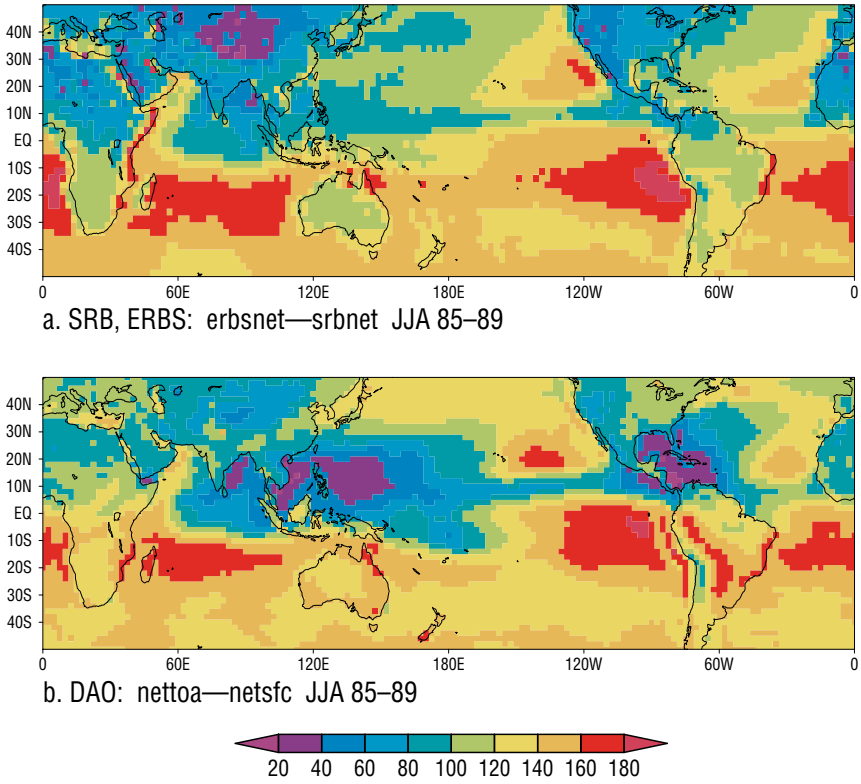

Figure 2. Warm season net atmospheric radiative cooling (W/m^2). (Top) Constructed by differencing ERBS top-of-atmosphere net radiation retrievals. (Bottom) As produced by GEOS-1 assimilation.

Analysis of MSU Data

(J. Christy—MSFC)

Considerable time was devoted to carefully analyze the possible effects of non-thermometric processes which might affect the MSU brightness temperatures. Progress was made in determining that the lower tropospheric temperatures do require slight adjustment due to instability issues so that the 18-year global lower tropospheric temperature trend in the new version "c" is -0.03 deg/decade rather than -0.06 deg/decade as in the old version "b". The stratospheric temperature for 1996 is the coldest yet observed as would be expected from record low values of stratospheric ozone.

Rapid changes in hemispheric and global temperature have been discovered in which the hemispheric mean lower tropospheric temperature might fluctuate by a full degree (C) in just 10 days. Such a perturbation requires considerable influxes or outfluxes of heat energy, most likely produced on this time scale by atmospheric hydrologic processes (eg. clouds). Efforts are underway to understand this short term climate sensitivity since its magnitude on the global scale is equal to several decades of anticipated global temperature warming due to the enhanced greenhouse effect.

Studies such as the Parker et al. (1996), which follow from the Christy and McNider (1994) work attempt to quantify global climate sensitivities to various forcing mechanisms (eg. volcanic aerosols, tropical SST variations) on monthly to annual time scales.

A 1 Km Multi-Layer Soil Characteristics Data Set for the Conterminous United States

(D.A. Miller, R.A. White, P.J. Kolb—PSU)

Information on soil properties is now widely required by climate and hydrology models and soil-vegetation-atmosphere transfer schemes. In 1996 we completed the first version of a multi-layer soil characteristics data set for the conterminous United States. This data set, CONUS-SOIL for short, specifically addresses the need for soil physical and hydraulic property information over large areas. The State Soil Geographic Database (STATSGO) developed by the United States Department of Agriculture-Natural Resources Conservation Service (USDA-NRCS) served as the starting point for CONUS-SOIL. Geographic information system (GIS) and Perl computer programming language tools (White and Miller, 1997) were used to create map coverages of soil properties including: soil texture and rock fragment classes, depth-to-bedrock, bulk density, porosity, rock fragment volume, particle-size (sand, silt, and clay) fractions, available water capacity, and hydrologic soil group. To provide maximum utility and flexibility, the CONUS-SOIL data sets are available in several formats with complete documentation over the ESSC WWW server. CONUS-SOIL became publicly available in the spring of 1996 and has been accessed by dozens of researchers throughout the United States as well as Europe and Asia. A manuscript describing CONUS-SOIL in full detail is nearly complete and will be submitted to the WWW journal Earth Interactions in early February 1997 (Miller and White, in prep).

Cloud and Precipitation Processes

A Convective-Stratiform Rainfall Classifier For Composite Radar Reflectivity Maps

(S. Goodman, R. Raghavan, P. Meyer, and D. Buechler—MSFC)

The objective of this study is to develop a data set to characterize rainfall fields from a multi-year data base of high spatial and temporal resolution radar reflectivity measurements. The radar reflectivity data product, referred to as NOWRAD, is composited in real-time from the U.S. National Weather Service network of WSR-57, WSR-74 and WSR88-D radars and provided to us by Weather Services, Inc. The spatial resolution of each pixel is 2 km over the United States with a temporal resolution of 15 minutes. Collaboration with Penn State involves producing 12-h continental rainfall fields as input to the soil hydrology model (SHM) to generate soil moisture fields. Initially Drs. Lakhtakia and Barros will use this product as input to their fine-mesh mesoscale models. After the methodology is well established, seasonal model runs will be used to assess the role of land-atmosphere interactions in modulating the interannual variability of rainfall.

The individual radar images are classified into convective and stratiform rainfall components. The integration of the 96 images received each day yields a daily rainfall estimate. These rainfall estimates are next integrated into monthly and seasonal estimates which are then to be used to examine the natural variability of rainfall in the United States from year-to-year during the period 1994–1996. Convective and stratiform rainfall regions are identified and then partitioned into convective and stratiform rainfall using two Z-R relationships.

A training data set using ten days in April 1994 was used to develop and test the methodology. Two case studies were then examined from rainfall episodes on 11 April 1994 and 21–22 April 1994 within the Arkansas-Red River Basin to assess the algorithm performance. The first objective was to establish a threshold function to select convective centers. Next, the gradient between each pixel and its neighbors was computed to isolate these centers. The neighborhood reflectivity was specified to be the linear average of non-zero reflectivities, Z, in a 100 km^2 region centered at any pixel. Finally the rainrate, R, in convective and stratiform rain areas is performed with $Z=300R1.4$ applied to the convective areas and $Z=200R1.6$ applied to the remaining rain areas.

Our initial attempt at classifying rainfall over one large river basin on a monthly time period is promising. Our 28-day sample data set for April shows low RMSE values of 0.12 mm (or 45% of the Stage-III area-averaged hourly mean rainfall) with a bias of 0.01 mm. It appears that the methodology should produce sufficiently accurate estimates of rainfall over large spatial domains and over multi-year time periods to characterize the year-to-year differences in rainfall. These rainfall distributions and characterizations can be used by MTPE scientists as input or validations to regional modeling experiments to learn more about the seasonal-to-interannual behavior of rainfall and its response to larger scale atmospheric forcing. This data base may also be of use in recomputing extreme rainfall statistics for improved water management models and decision aids.

A Model Of The Transition From Stratocumulus To Trade-Wind Cumulus Clouds

(S. Wang—MSFC)

Recent modeling and observational studies have provided new physical insight into the problem of the transition from stratocumulus to trade-wind cumulus clouds. It has been found in many studies that decoupling in the boundary layer and cumulus clouds play crucial roles in the processes leading to the breakup of stratocumulus clouds. Based on these new understanding, a parameterization has been developed that can realistically simulate both stratocumulus, trade-wind cumulus and the transition between them. The model has the following features: a second-order turbulence closure model, a shallow cumulus transport scheme with a simple representation of cloud-top entrainment and a cloud scheme that predicts both liquid water content and cloud fraction with detrainment from cumulus updrafts as a major source. When decoupling does not occur, the model operates as a typical turbulence closure model with a turbulence subgrid-scale condensation in a predictive mode. After the decoupling criteria is met, the cumulus scheme is turned on with a full prognostic cloud scheme.

The model has been used to simulate the downstream development of a boundary layer column along the trajectory of the lower branch of Hadley circulation. Reasonable estimates of the cloud fraction and liquid water content were obtained. In addition, the transition zone is also simulated. In the transition region, the cumulus transport acts as a major moisture source to the cloud layer, while environment turbulence from the second-order closure model is a sink as a result of boundary-layer top entrainment. However, the cumulus transport is never enough to make up the loss to the environmental turbulence. It results because the cumulus induced cloud-top entrainment tends to make the environment less moist; and penetrative cumulus updrafts bring much of the moisture into the inversion instead of the cloud layer. Liquid water deposited in the inversion layer is therefore rapidly evaporated. The interaction between environment turbulence and cumulus transport leads to the breakup of the stratocumulus clouds. In addition, cumulus clouds transport moisture out of the subcloud layer to limit the accumulation of moisture. Without a cumulus scheme, the turbulence moisture flux undergoes periodic bust resulting from saturation at the top of the subcloud layer, leading to a strong oscillation in the cloud field and preventing a long lasting breakup of stratocumulus. Thus incorporation of shallow cumulus convection in a turbulence closure model is essential in simulating the transition. This work was summarized in a presentation of the 1996 AGU Fall meetings (Wang, 1996). Currently, the formulation of cumulus-induced entrainment and the prognostic cloud scheme are being refined.

Multichannel Single Spectrum Analysis of Climate and Hydrology Elements

(T.-Y. Shun and C. Duffy—PSU)

Our goal is to isolate the periodic components and characterize the space distribution of runoff, precipitation and temperature in a mountainous region. Compared with classical spectral analysis, where the basis functions are continuous (e.g. sines and cosines), the multichannel single spectrum analysis (MSSA) allows the direct evaluation of the basis functions from sampling datasets and couples space and time in data patterns simultaneously. The low frequency (interdecadal period) for the monthly runoff field is found and dominates in the low elevation area. This result shows that there might be the discharge of groundwater into runoff at the lower elevation area on a mountain front. The annual and seasonal cycles are found among all three climatic fields. For the precipitation, the amplitude of the harmonics increases with the elevation, whereas the amplitude of the harmonics decreases with the elevation. However, no simple rule about the relationship between the frequency of the runoff and elevation exists. Next, the relationship between runoff, precipitation and temperature are studied. By using MSSA, the optimal reconstruction of a dynamic process at space and time can be provided. The runoff-precipitation-temperature trajectory in the Wasatch Range was examined and interpreted (Shun and Duffy, 1996).

Stochastic Resonance and Nonlinear Groundwater Reservoirs

(C. Duffy—PSU)

A possible link between small amplitude, low frequency, periodic components in long-record precipitation time series which apparently lead to large amplitude fluctuations in stream runoff at the same forcing period has been studied. The phenomenon has recently been observed in mountainous drainage basins of the Wasatch range which is the source-area for the Great Salt Lake. The interpretation is based on the now widely used concept of stochastic resonance (SR). The usual condition for SR is a weak periodic signal embedded in stochastic noise, which serves as forcing to a nonlinear dynamical system. The noise induces resonance when the deterministic and stochastic time scales of the system become commensurate. The groundwater is important to streamflow since it introduces nonlinearity in the storage-flux relation and introduces the necessary range of time scales. Both the nonlinearity and the time scales depend on the geometry and altitude of the reservoir. A two-state model is proposed where high elevation groundwater storage reservoir is coupled with a low elevation mountain-front reservoir via two paths: deep slow-flow through the fractured and porous mountain and basin rocks and sediments, and a fast surface flow which is initiated when a critical value of storage is exceeded.

Susquehanna River Basin Experiment (SRBEX)

Introduction

SRBEX is the first of several planned regional experiments which are to be undertaken in our EOS research program. The Susquehanna River Basin (SRB) is a 62,419 km^2 watershed covering portions of New York, Pennsylvania, and Maryland (Figure 3). The overarching goals of SRBEX are to understand the hydrologic cycle of the basin through modeling and the analysis of observed data, and as a result of this understanding to develop capabilities for monitoring and projecting changes in basin hydrology. The reason for SRBEX is clear: accurate projections mean that managers will be able (1) to lessen the impacts of variations in water quality and supply and (2) to optimize water resources. Thus, significant social and economic costs can be avoided and benefits can be realized by the research efforts of SRBEX.

More specifically, SRBEX includes the following policy-relevant objectives:

1. Identification of hydrologic parameters sensitive to climatic variation and change
2. Model experimentation to provide quantitative comparison of the hydrologic system sensitivities to various natural and human forcing functions
3. Observational studies to provide the context for comparisons of natural versus human-induced variations

Figure 4 summarizes the SRBEX suite of databases, data sets, and linked models.

Coupled Global-Regional Climate Model Simulations

(E. Barron and G. Jenkins—PSU)

The nesting of GCMs, mesoscale models and terrestrial hydrologic models is now proceeding rapidly. Research on this topic is moving simultaneously in three distinct phases. The first major effort involves coupling of GCMs and mesoscale models. The second major element includes using an observation-driven mesoscale model coupled with a terrestrial hydrologic model to predict hydrographs for the Susquehanna River. The third element focuses on a fully nested strategy in which predictions for the Susquehanna River are independent of the meteorological observations.

Eric Barron and Greg Jenkins have completed a series of experiments to assess and improve the capabilities of the coupled GCM-Mesoscale Model methodology. Last year, assessments were completed to determine whether long-term simulations were feasible and to determine the significance of Mesoscale model domain size in the quality of precipitation prediction (Barron et al., 1996; Jenkins and Barron, 1997a). Long-term simulations proved to be feasible, and it was demonstrated that the nested model produced a substantially improved precipitation forecast in comparison with the stand alone GCM. In addition, a continental-sized mesoscale model domain proved to provide a better simulation than a domain chosen only on numerical considerations.

Following these results, three long nested GCM-Mesoscale Model simulations have been completed. First, a ten year AMIP (1979–1988) experiment, with time-varying sea surface temperatures, was executed. The results further demonstrated that the nested methodology resulted in substantially improved predictions of United States precipitation compared to the stand-alone GCM. Figure 5 illustrates both the GENESIS AMIP GCM results for precipitation and the observations for 1979 to 1988. The tendency for GENESIS to over predict precipitation and to miss some of the regional precipitation structure is evident. In comparison, Figure 6 gives the results of the mesoscale model (RegCM2) nested with the GENESIS simulation. Significant improvements in both the pattern and amounts of predicted precipitation can be noted in comparison with the observations (Peterson et al., 1995; Barron et al., 1996; Jenkins and Barron, 1997b; Barron and Jenkins, in prep). These results add confidence to our application of the nested model strategy as a means of achieving higher spatial resolution simulations without the computational costs of global, high resolution simulations. Interestingly, the noted improvements in the precipitation were not matched in other variables which describe the atmospheric dynamics simulated by the models (e.g. geopotential height field, 200 mb winds, etc). These fields closely mimicked the results of the GCM. This fact suggests that the improvements in precipitation prediction stem from the increased spatial resolution of the topography and better precipitation physics, and not to a dramatically improved simulation of the atmospheric circulation at higher resolution. These results suggest that the evaluation of statistical techniques for downscaling (see later section) may also be a valuable approach to improving precipitation predictions.

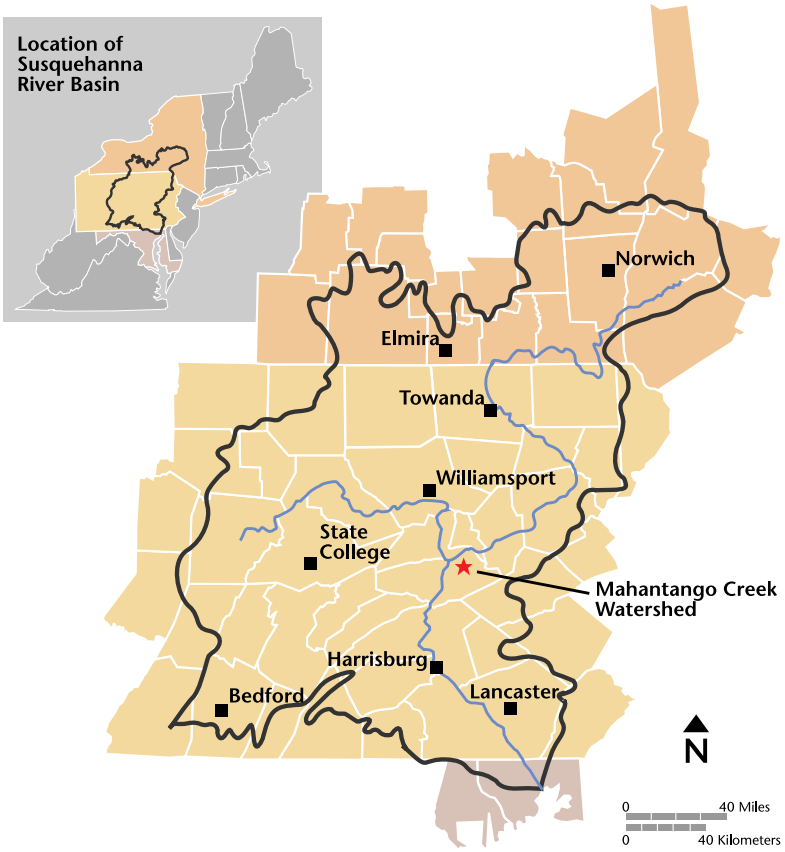

Figure 3: The Susquehanna River Basin

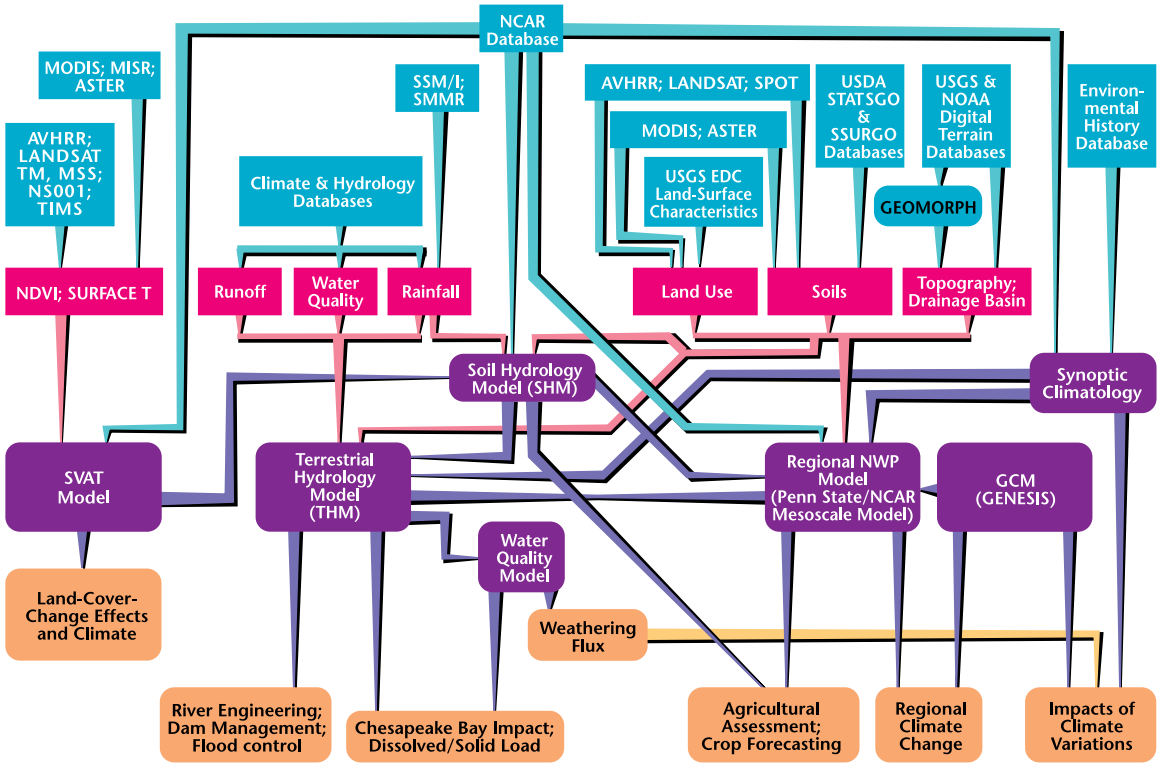

Figure 4: The structure of the Susquehanna River Basin Experiment (SRBEX)

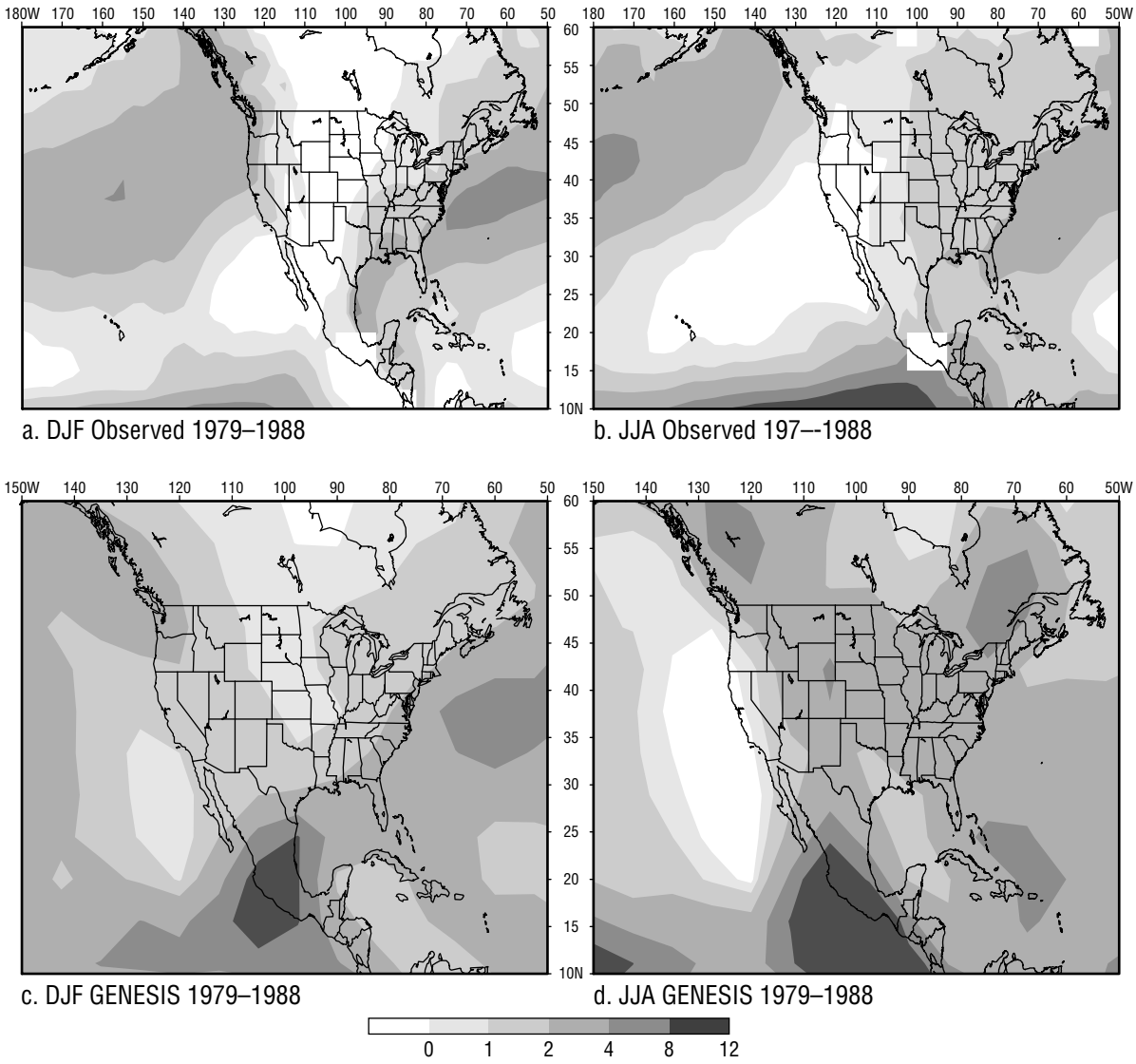

Figure 5. Precipitation Rates for DJF and JJA 1979–1988. GENESIS simulation use observed SSTs. Units in mm/day.

The AMIP runs also illustrate a flaw in the simulations. The interior of the continental U.S. and a portion of the western U.S. were consistently predicted to be too warm in summer compared to observations. Comparisons with observations indicate that the simulated cloud cover amounts were too low, and that soil drying resulted in too warm a summer surface temperature. Similar results were noted in several other nested GCM-mesoscale models presented at a recent conference on High Resolution Climate Modeling in Wengen, Switzerland. The consistency of the results points to a scaling issue with regard to cloud physics or surface fluxes.

Barron and Jenkins (1995) and Jenkins and Barron (1997b) examined specifically the period of the 1988 summer drought, and the ability of the nested model strategy to capture this event. In a case in which RegCM2 was driven by observations, the 1988 drought was well simulated. In the case where RegCM2 was driven by the GENESIS AMIP experiment, the timing and the magnitude of the 1988 drought were not well simulated. Both the GCM and ECMWF analyses produced a

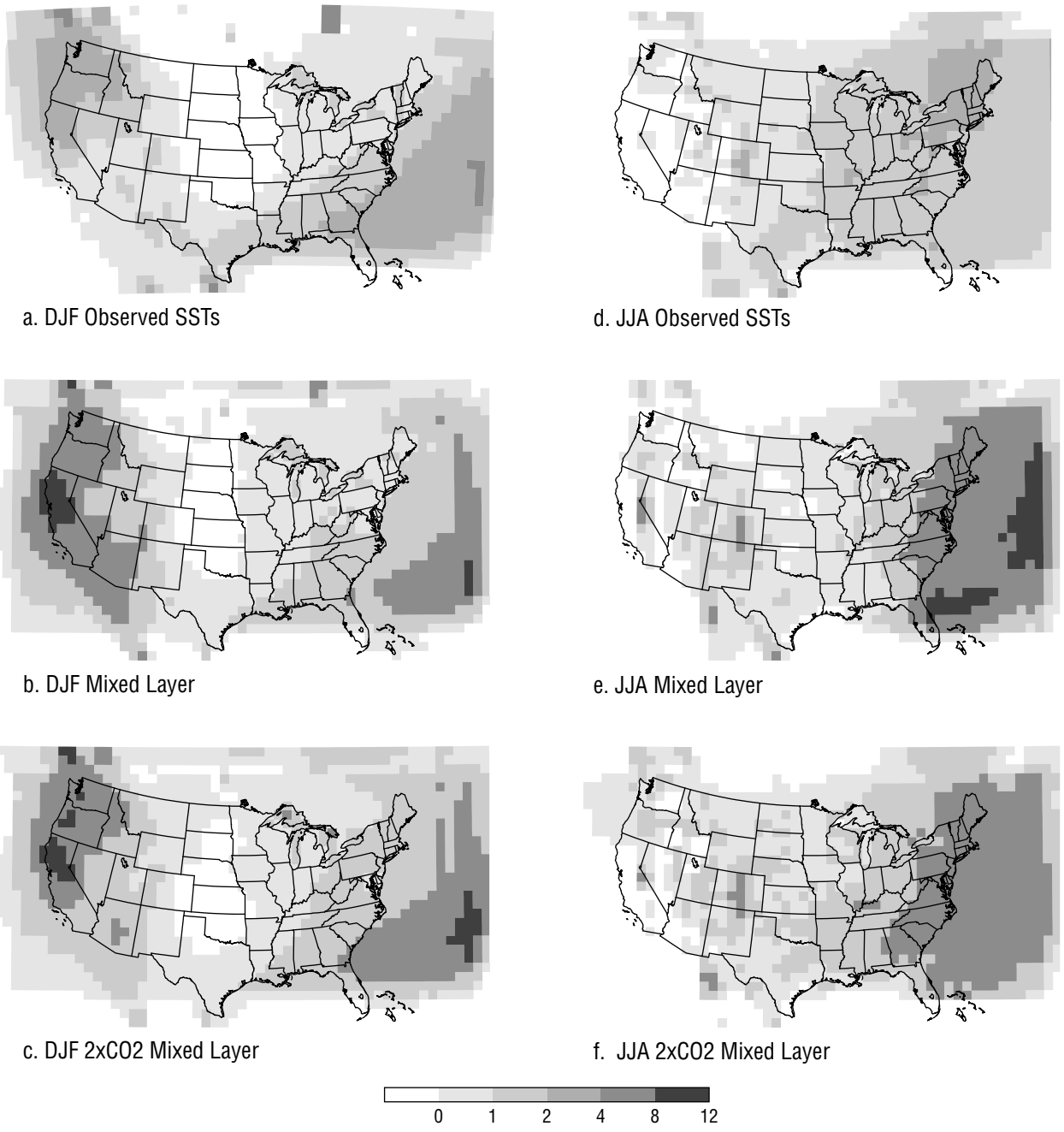

Figure 6. Precipitation Rates for DJF and JJA using the nested regional climate model. Units in mm/day.

summer drought, but the GENESIS-driven experiment produced the driest and warmest periods in August of 1988, rather than June. The results are directly tied to the GENESIS simulation of the planetary wave pattern. On average over the ten year AMIP period, GENESIS provides a reasonable simulation of the atmospheric circulation. However, for individual seasons, the GCM simulation may introduce errors even at the larger scales.

Second, Barron and Jenkins completed two nested model experiments in which sea surface temperatures in the GCM were calculated using a mixed layer ocean model with specified ocean heat transport (as opposed to the specified, annually varying AMIP SSTs). The first experiment was for the present day (Figure 6 b and e). The precipitation prediction from the mesoscale model driven by the mixed layer GCM is substantially poorer than in the AMIP experiment. In

particular, the western and southwestern U.S. precipitation is substantially greater than observed in December-January-February, and the eastern U.S. precipitation is greater than observed in June-July-August (Figure 6a and d). The lack of realistic structure to the ocean SSTs has resulted in a poorer simulation of the planetary scale waves in the GCM and significantly different coastal ocean temperatures than observed. This suggests that coupled ocean-atmosphere simulations, which can achieve a reasonable surface temperature structure, are likely to result in significant improvement.

Barron and Jenkins also completed a nested model experiment in which sea surface temperatures in the GCM were calculated using a mixed layer ocean model in which the atmospheric carbon dioxide concentration was doubled (Figure 6 c and f). The nested model experiment for doubled carbon dioxide resulted in less precipitation in the southwestern part of the U.S. in winter and a somewhat wetter winter in the northeast. In summer, the two model experiments are highly similar in terms of precipitation with the exception that the southern U.S. has higher precipitation than the present day experiment. However, the comparison of these two mixed layer GCM experiments and their resultant mesoscale model experiment must be viewed as sensitivity experiments because the differences between the present day AMIP and mixed layer experiments is greater than the difference between the mixed layer experiment with present day carbon dioxide and the experiment with doubled carbon dioxide. Again this result emphasizes the importance of the ocean surface temperature distribution in nested GCM-mesoscale model results.

Synoptic Climatology and Downscaling

(R. Crane, B. Yarnal, B. Hewitson—PSU)

Doubled CO_2 Precipitation Scenarios for the Susquehanna River Basin

Given the limitations of GCM grid-point predictions, and the necessity for high resolution (regional) data, there has been a growing interest in the concept of downscaling: developing techniques for extrapolating from the GCM scale down to the regional scale of interest to other social and environmental scientists. One approach is to utilize empirically derived transforms that relate larger-scale features of the GCM to regional climate values. Karl et al. (1990) and Wigley et al. (1990) describe methodologies for deriving empirical relationships between local climate variables and the same suite of variables from the GCM simulations. This approach is analogous to techniques used in numerical weather forecasting where the large-scale data are regarded as being correct, and the approach is simply to take the value obtained from observation, or a model, and use the empirical function to distribute that parameter across a higher resolution grid.

Here we describe a slightly different approach for deriving sub-grid-scale precipitation from GCM simulations. This approach ignores the actual grid-point values simulated by the model (because of the skill problems noted earlier), and uses artificial neural nets (ANNs) to derive transfer functions between the larger-scale atmospheric circulation and the local climate. This is similar to the approach described by Hewitson and Crane (1992a), which examined circulation-temperature relationships over the U.S. using a polynomial regression model to derive the transfer functions, and it expands on an earlier neural net based study of circulation-precipitation relationships conducted for a tropical region of southern Mexico (Hewitson and Crane 1992b). The present methodology differs from the earlier studies in that specific humidity at three atmospheric levels is also added as an input to the neural net. Such an approach is predicated on the condition that there is a clear relationship between the larger-scale atmospheric state and the local precipitation, and that the GCM produces an accurate simulation of the atmospheric circulation and humidity fields at the scale used for the analysis. Our research shows that these condi-

tions are met for the Susquehanna region of the eastern United States in a present-day simulation from version 2 of the GENESIS climate model. Climate change scenarios are produced by applying the same downscaling transfer function to a doubled CO_2 version of the GENESIS model.

The observational data used to develop the cross-scale relationships are from the Goddard Space Flight Center's (GSFC) eight year data assimilation (3/85–2/93).The data set was based on the full extent of observational data available and used the GSFC GCM to produce a twice daily gridded data set at a resolution of 2° latitude by 2.5° longitude. These data are included in the Earth Observing System (EOS) Data and Information System (EOSDIS), and are available through the GSFC Distributed Active Archive Center (DAAC). The gridded 1000 mb and 500 mb geopotential heights were extracted for a window encompassing the Susquehanna basin, extending from 35°N to 47°N, and from 83.75°W to 68.75°W (Figure 7). Specific humidity at 1000 mb, 700 mb, and 500 mb, and precipitation were extracted on the same grid for the 4x4 box of grid cells surrounding the Susquehanna basin (Figure 7).

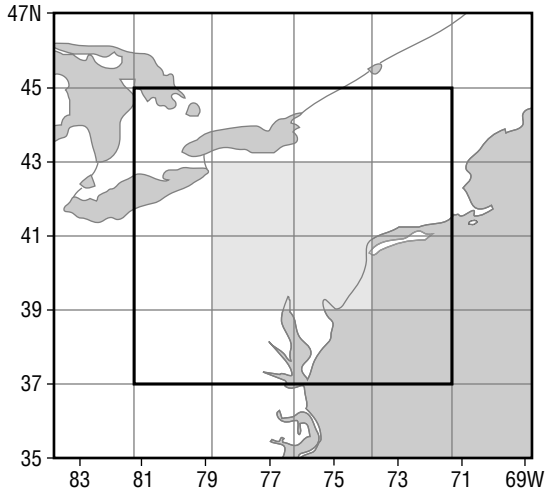

Figure 7. Location map showing the GSFC cells used in the analysis. The Susquehanna River Basin lies within the shaded region.

Six years of GCM data used were obtained from a control simulation of version 2 of the GENESIS GCM (Thompson and Pollard, submitted) run at T31 resolution. Following a 12 year spin-up period, the daily data for six years of equilibrium climate simulations were extracted for the same atmospheric window as the observational data.The GCM data were regridded to the same 2°x2.5° grid used for the GSFC data.The interpolation was performed with a linear inverse square interpolation procedure using spherical distances and accounting for directional bias in the data point distribution (see Wilmott et al., 1985).

The independent variables (inputs to the ANN) are time-lagged GSFC 1000 mb and 500 mb heights for the nine grid cells centered on the target cell (the grid cell for which the precipitation is to be derived), together with the 1000 mb, 700 mb, and 500 mb specific humidities for the target cell.The precipitation is "predicted" for the 0000z observation period using input data for 0000z, the two preceding 12-hourly observations, and 1200z the following day. The day of the year is included as an additional input, using the sine of the date, where the date is expressed in terms of 360°/year.The dependent variable (ANN output) is the daily precipitation for the target grid cell.Thus, for each grid cell 84 circulation and humidity inputs are used as predictors, along with the date, and the ANN is trained to predict daily (0000z) precipitation amounts.The ANNs were trained using a standard backpropagation algorithm on the first 75% of the days (2192 days) while retaining the last 25% as an independent test set.

Once trained the ANN is used with all days in the test and training data set to generate daily precipitation as a function of the atmospheric forcing. This is a *generalized* relationship in which the ANN has learned the general state and temporal sequence of the atmospheric circulation in relation to the differing precipitation amounts. The correlation between the observed and neural net predicted precipitation over the 16 cells ranges from 0.60 to 0.84 with daily mean absolute errors of 1–3 mm. Figure 8 shows the observed precipitation (mm/mth) obtained from the GSFC data set, the downscaled precipitation derived from the GSFC circulation and humidity data, and the precipitation values from the nearest GENESIS grid cell. The data are for the four GSFC grid cells that encompass the Susquehanna Basin. The downscaling procedure effectively captures the seasonal cycle and the monthly precipitation totals, but with a tendency to over predict low precipitation events in winter and under predict high events in summer. Figure 8 also shows that the precipitation produced in the GENESIS cell that covers the southern two GSFC cells also matches the observed seasonal distributions, but with greater errors than the downscaled data. The northern GENESIS cell, however, completely fails to match the seasonal cycle and produces far too little summer rainfall—further illustrating the problem of using individual GCM grid cell values for climate analysis.

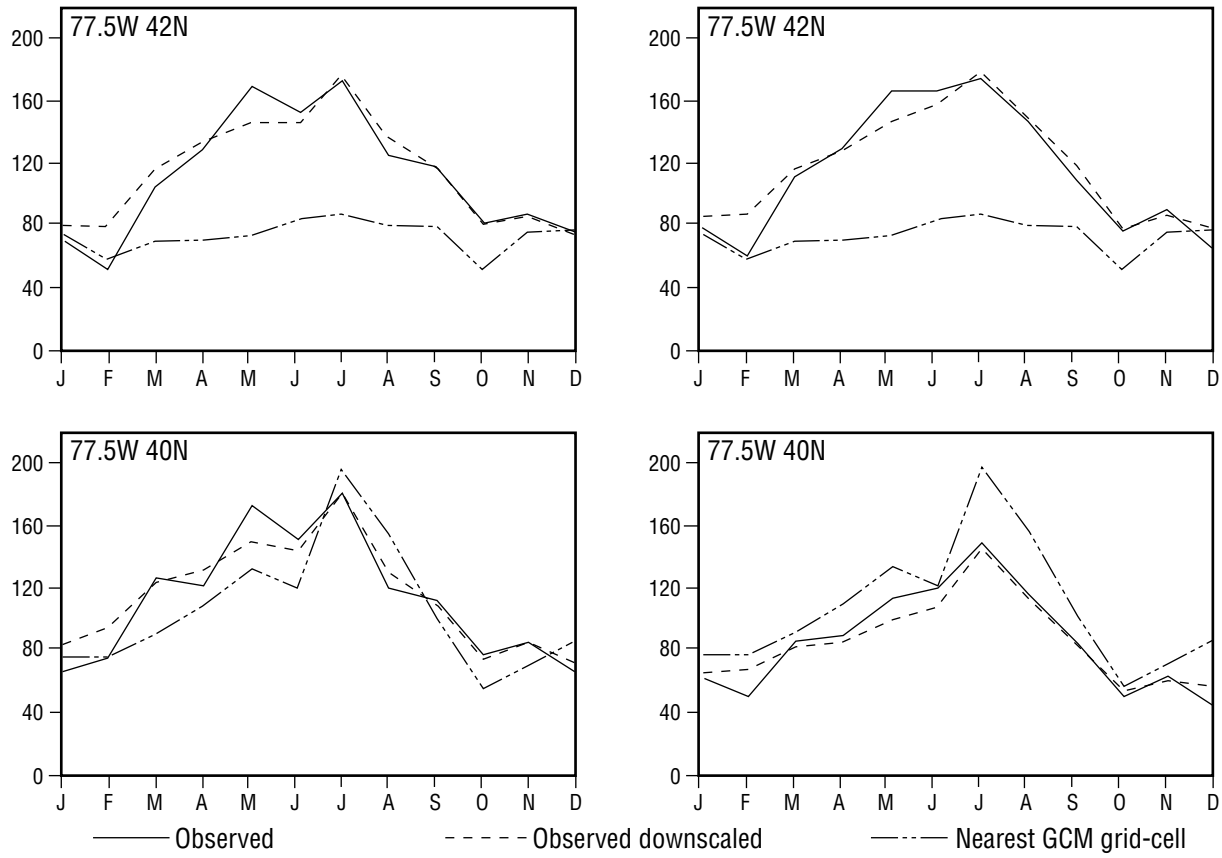

Figure 8. The downscaled precipitation (mm/month) for the four grid cells highlighted in Figure 7. For each grid cell the downscaled precipitation is compared to the observed precipitation and the precipitation produced by the nearest GENESIS grid cell.

Data from a 1xCO_2 and 2xCO_2 version of the GENESIS model (using the same land surface model) are input to the neural nets to calculate the change in precipitation that will occur due to changes in circulation and humidity patterns in a doubled CO_2 climate. Figure 9 shows monthly precipitation totals (mm/mth) for the four 2°x2.5° GSFC grid cells encompassing the Susquehanna Basin. The graphs show results from the 1xCO_2 and 2xCO_2 model runs, using both the actual GCM output as well as the downscaled precipitation. The downscaled response over all four cells is very similar with each showing a substantial increase in precipitation, particularly in the spring and summer months. The total cumulative precipitation from April through September increases by 32% when averaged over all four grid cells (Table 1). This picture is very different to what one sees when examining the actual GCM precipitation fields. Although the GCM shows a general increase in precipitation in this region for a doubled CO_2 climate, it fails to capture the magnitude of the change anywhere except for the southeast portion of the Basin.

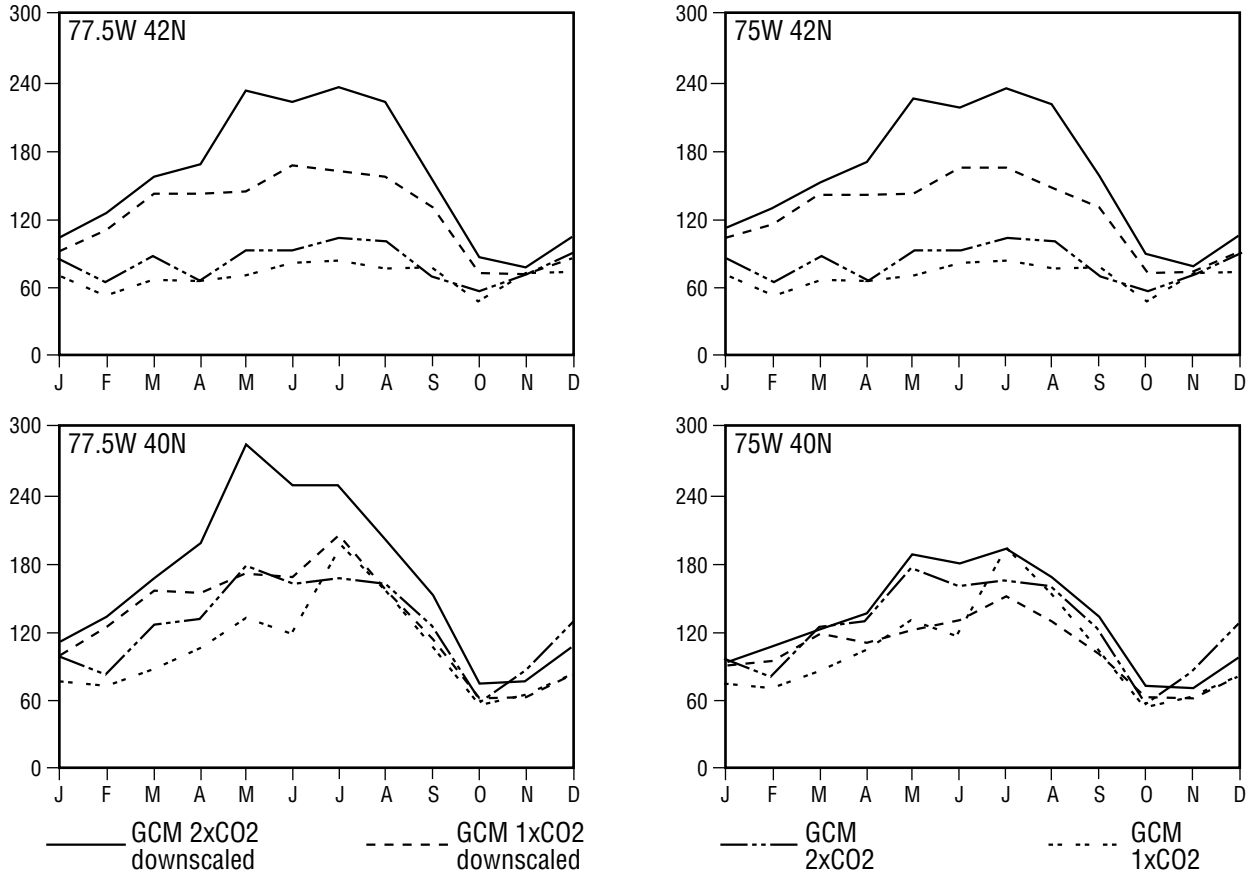

Figure 9. The actual and downscaled precipitation (mm/month) projections from the single and doubled CO2 climate model for the four grid cells highlighted in Figure 7.

Regional Synoptic-Scale Atmospheric Circulation

Earlier research using synoptic climatology to identify and analyze representative discharge events in the Susquehanna River Basin (Frakes and Yarnal, 1996a; Frakes and Yarnal, 1996b; Yarnal and Frakes, 1997a) evolved with the development of computerized pattern-recognition algorithms to extend and objectify the methodology (Frakes and Yarnal, 1996c). These algorithms were then used to construct a long-term climatology of the region's synoptic-scale atmospheric circulation (Yarnal and Frakes, 1997b).

	J	F	M	A	M	J	J	A	S	O	N	D
1xCO2	91.5	96.8	121.7	113.2	123.5	132.3	153.7	132.2	105.0	67.2	64.2	85.3
2xCO2	93.4	106.8	120.8	135.0	186.9	180.8	193.4	169.7	134.1	73.7	70.4	97.7
Change	1.9	10.0	0.9	21.8	63.4	48.5	39.7	37.4	29.1	6.5	6.2	12.4
% Change	2.1	10.3	0.7	19.2	51.3	36.6	25.8	28.2	37.2	9.6	9.6	14.5

Table 1. Monthly precipitation totals averaged for the 4 grid cells encompassing the Susquehanna River Basin (mm).

Scaling Issues and Long-Term Simulation of Water and Energy Budgets at the Land-Surface

(A. Barros, R. Bindlish—PSU)

The purpose of this work is to develop and evaluate physically-based approaches to downscaling climate model output for long-term simulations of water and energy budgets at the land surface. The objective is to use these data and tools to determine the impact of climate variability on regional water resources, and to investigate the linkages between the frequency and magnitude of extreme events such as floods and droughts and climate phenomena.

Initial research has focused on: (a) aggregation and disaggregation of terrain and land surface properties, and downscaling of rainfall; (b) modification of an existing land-atmosphere interactions model to include radiation and runoff routing schemes; (c) data analysis of hydrological and climate data to identify the relationship between macroscale hydrology and climate forcings, such as ENSO, in the context of extreme hydrologic events.

A model for the aggregation and disaggregation of distributed variables based on the preservation of the spatial properties and textural arrangements of the data (e.g. terrain) was developed and evaluated (Bindlish and Barros, 1996a). The model has also been applied to evaluate the scaling properties of remote sensing imagery of soil moisture and to evaluate the propagation of uncertainty in the specification of soil properties for modeling studies at different scales (Barros et al. in prep.; Bindlish and Barros in prep.). Ongoing work consists of comparing the downscaled rainfall fields obtained from the SRBEX storm simulations using this approach and the results obtained using a physically-based disaggregation approach (Barros, 1995).

A land-surface model built upon the land surface parameterization used in the ECMWF model and used in previous studies has been modified to include a radiation module. Model performance was evaluated for the Cabaw data (R21), which is a revised version of the data set used previously in PILPS. The model has also been equipped with a modified runoff routing scheme imported from the Terrestrial Hydrology Model (THM) used in SRBEX. Currently, distributed-model simulations are being prepared for the West Branch of the Susquehanna River Basin. The implications of using distinct downscaling approaches will be investigated with regard to streamflow response and soil moisture distribution at a range of scales.

The existence of coupled modes of variability of the land-atmosphere-ocean system connecting hydrologic phenomena to specific climate forcings such as ENSO is being investigated using functional texture analysis. This methodology, based on image processing techniques, provides quantitative measures of the space-time structure and evolution of spatial variables. In particular, an intercomparison study of the ISCCP C2 data set and model output from GENESIS and CCM2 was conducted to evaluate how the GCMs replicate change over time of cloud cover, temperature and precipitation fields as described by homogeneity, contrast, order and spread measures (Bindlish and Barros, 1996b). Preliminary research for the 1986 flooding and 1988 drought in the

Mississippi basin suggests that large-scale flooding and drought episodes over the continental U.S. can be predicted 9-18 months in advance by the concerted monitoring of the time-rate of change of these functional measures and ENSO indices.

Penn State/NCAR Mesoscale Model (MM)

(M. Lakhtakia, W. Capehart—PSU; W. LaPenta—MSFC)

The Penn State/NCAR Mesoscale Model (MM) is a versatile three-dimensional, limited-area meteorological numerical model. MM5 is nonhydrostatic and it permits the use of multiple nested domains, which allows for the dynamically consistent downscaling from the global scale of the GCM to the local scale of the Terrestrial Hydrology Model (THM). It also includes efficient numerics to make longer-range simulations less time consuming. All these features make MM5 an excellent choice for studying regional climate changes with emphasis on the water cycle.

Version 1 of MM5 (MM5v1) was officially released for public use in February 1994. The entire MM5 system (including pre- and post-processing programs) was transferred to the Penn State, and the necessary changes and tests to run those programs on that platform were made. Among these changes is the inclusion of a sophisticated soil surface-vegetation-atmosphere transfer scheme (a modified version of the Biosphere-Atmosphere Transfer Scheme [BATS] [Lakhtakia and Warner, 1994]). This is the version of the model used for the ongoing SRBEX work, i.e., the single-storm simulations and the linkage of the Soil Hydrology Model and MM5, which are discussed later on in this document.

One of our scientific goals is to develop a modeling system that can accurately project basin runoff on seasonal to interannual time scales. The ultimate model development goal is to evolve MM5 to the point where it replaces RegCM2 (which is based on MM4) as a mesoclimate model that can be linked to the General Circulation Model. That is, we need to develop a non hydrostatic mesoclimate model capable of operating at relatively fine spatial and temporal resolutions. To reach these goals, we will need to modify MM5 accordingly. The following is a list of the required ongoing or near-future modifications to MM5:

1. Move to MM5 version 2 (MM5v2), which was released in the Summer of 1996. This change is being prompted by two different reasons: a computing one and a scientific one. The computing reason is based on the changes that are going on in the Cray computing environment. Cray is phasing out the tools that have been used for many years to manage the Mesoscale Model source code, as well as the compiler interface (cf77). Instead, the "programming environment 2.0" and a newer compiler interface (cf90) will be the default. MM5v2 has been built specifically for the new programming environment.

   MM5v2 has some features that are very desirable for long-term simulations. For instance, MM5v2 includes alternative atmospheric radiation packages that should be used when performing mesoclimate simulations. We have already transferred MM5v2 to the Penn State and will start using it in early 1997.

2. Move the BATS code from MM5v1 to MM5v2. Lapenta has taken the Penn State modified BATS version within MM5v1 and moved it into MM5v2. Initial tests seem promising. LaPenta and Capehart are working to validate the model at the CART-ARM study area. An effort is underway at MSFC to validate the surface energy budget of the coupled MM5/BATS modeling system using in situ observations collected during the Atmospheric Radiation Measurement (ARM) Program. The initial phase of the effort focuses on July 7, 1995 over the Southern Great Plains

Cloud and Radiation Testbed (SGP/CART) during the Surface Energy Exchange IOP. Clear sky conditions prevailed over the region on this day thus limiting cloud effects on the surface energy balance. The model was modified to output specific terms within the surface energy budget so that they may be directly intercompared with in situ observations obtained from ten sites. Observed variables available at thirty-minute intervals include sensible and evaporative fluxes, net radiation (obtained from Energy Balance Bowen Ratio Stations), near surface air temperature, specific humidity, wind speed and direction (obtained from Surface Meteorological Observing Stations). A non-nested grid configuration was chosen for initial testing with a modest horizontal resolution of 36-km. The first 24-h integration revealed several inconsistencies existed in the coupling between BATS and MM5 which were effectively identified and corrected. Preliminary results with the updated system indicates the coupled model produces a realistic diurnal cycle at all ten sites. A 36-h simulation was performed using a 1-way nested configuration with the coarse domain having a 36-km resolution with a 12-km nest. Preliminary results show that near surface air temperatures without BATS are under-predicted by as much as 6°C over south-central Kansas after 33-h (Figure 10). A detailed intercomparison between EBBR data from the ARM-CART sites and model output is currently under way to investigate differences in the surface energy budgets of the two models. The CART-ARM data set includes surface flux measurements that can be used to validate those fluxes calculated by BATS. Since the SGP Site is within the Real-Time MM5 domain SHM-derived soil-water content may be used to initialize the soil moisture within BATS with little difficulty. Validation studies will use both MM5-determined values of soil moisture and those calculated by SHM.

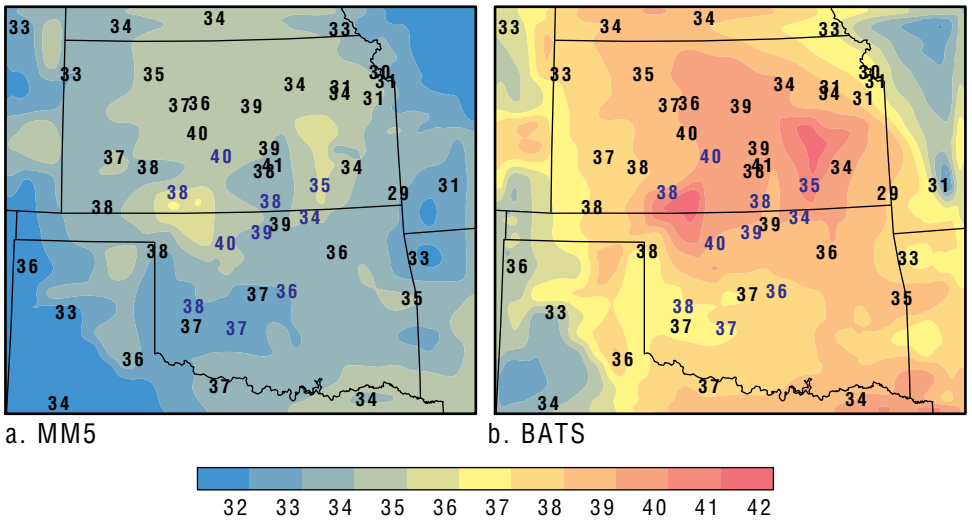

Figure 10. 33 hour simulated air temperature (C) valid at 2100 UTC 8 July 1995 on a 12-km nested domain for MM5 using the Blackadar PBL coupled with (a) the standard force-restore surface energy budget and (b) BATS. Observations overlain in black represent the standard NWS reporting stations while those in blue represent the ARM-CART sites.

3. Additional ongoing effort at MSFC involves the implementation of a satellite assimilation technique within MM5 that will provide an alternative dataset to validate the MM5/BATS system. It is well known that the coupling between surface radiation, hydrology, and surface energy transfer is very complex and requires the specification of additional parameters within the modeling framework, such as root-zone moisture, vegetative resistances, and soil moisture at the surface. Since measurements of such parameters are not routinely available, this presents a problem when initializing and validating numerical models. As a result, McNider et al. (1994) have formulated a simple technique for assimilating satellite-observed surface skin temperature (from GOES) into a mesoscale model in an energetically consistent manner that avoids having to specify some of the more difficult-to-define parameters discussed above. The technique explicitly assumes that the availability of moisture (either from the soil or vegetation) is the least known term in the surface energy budget. The atmospheric model surface parameterization is forced with surface skin-temperature heating rates, rather than absolute magnitudes of remotely sensed skin-temperature. This has the benefit of eliminating the systematic bias due to sensor errors and view angle.

   Significant progress has been made on implementing the technique within the MM5 model. An attempt is currently underway to replicate results published by McNider et al. (1994) for a test case over the Oklahoma region. Once completed, we will apply the assimilation for the July 7, 1995 case so that direct intercomparisons of the observed and simulated surface energy budgets produced by the assimilation and MM5/BATS model configurations can be performed. The GOES data for July 7 have been collected and processed at MSFC and is currently available.

4. The MM5/BATS at PSU/ESSC is currently integrated for periods not exceeding 24-h. It is our intent to perform longer term simulations (on order of several weeks) with a grid covering the continental United States and forcing the model with lateral boundary conditions generated from observed data. Our period of interest is the Summer of 1996, which was characterized by severe drought conditions across the Southern Plains and Southwest and well above normal rainfall in the Northeast. The basic precipitation pattern developed in October 1995 and generally persisted through Winter, Spring, and Summer 1996 with only a few significant breaks (most notably late May and late August). This corresponded to the persistence of upper-level ridging (northward displacement of the jet stream) over the West, and upper-level troughing (southward jet-stream displacement) through the Great lakes and the Northeast.

5. Additional programming tasks are underway, such as making the required changes in the RegCM2 pre-processors to create the initial conditions in the format required by MM5.

Soil Hydrology Model (SHM)

SHM Mesoscale Model Linkage

(M. Lakhtakia—PSU)

Regional-scale atmospheric models require the initialization of soil-water (SW) variables for various soil layers over the horizontal model domain. Routine SW measurements over large areas

(like the ones typically covered by regional-scale model domains) are unfeasible. The alternative use of climatological estimates of SW may result in large errors during periods of excessive rainfall or drought. Therefore, an indirect method is needed to determine SW fields from routine meteorological observations.

The indirect method used in SRBEX makes use of a one-dimensional SW diffusion and gravitation scheme (the Soil Hydrology Model [SHM], developed by Capehart and Carlson [1994]) to determine the temporal evolution of the vertical profile of SW. SHM is driven entirely by routine meteorological observations at the surface (i.e., the atmospheric forcing: air temperature, moisture and wind speed, as well as cloud cover and precipitation), information on soil and land cover characteristics (soil texture, land cover type, and fractional vegetation cover), and terrain slope.

SHM is initialized with an arbitrary SW profile. Driven by the atmospheric forcing, it converges toward a common solution regardless of the initial SW value. This convergence takes place over a period ranging from a few weeks to a couple of months, depending on the precipitation amounts. This period of adjustment is called the "balancing" period.

In order to use SHM to provide SW initial conditions for BATS in MM5, SHM must be applied to each grid cell over the entire MM5 domain. Smith et al. (1994) developed and tested this procedure for a historical case. SHM was modified so that it uses the same soil and land cover characteristics as BATS.

To test the effect of SHM in providing initial fields of SW for the land-surface component of MM5, we have developed a real-time version of the SHM system (rtSHM), which provides up-to-date SW fields to MM5 (Lakhtakia et al., 1994a, b). This system updates the SW fields generated by SHM on a daily basis and makes them available to the real-time MM5 (rtMM5). After a couple of months in operation, the rtSHM output can be assumed to be balanced, and, as a result, it may be used as initial conditions to MM5. This allows for real-time testing of the SHM-system capabilities. Testing includes MM5 simulations, using climatological values of SW as well as the rtSHM-simulated SW fields as initial conditions, and comparison of the predicted afternoon temperature and specific humidity close to the surface with observations.

A Real-Time SHM System to Produce Soil Water Fields for Real-Time MM5

(M. Lakhtakia—PSU)

Within the last year, development or, in some cases, modification, of the different modules required to make SHM operational using real-time meteorological information, as opposed to historical information, has been carried out. The resulting rtSHM became operational in mid-February 1996 (Figure 11). The link between the rtSHM and rtMM5 has also been developed. Since both models and their link became operational, a few numerical simulations have been performed using different setups of both models, starting in the late Spring of 1996.

The geographic domain used by the linked rtSHM and rtMM5 is shown in Figure 12. The real-time meteorological data (referred to as the "Analyzed meteorological information" and the "Surface meteorological information" in Figure 11) are read and formatted for the real-time model grid. All of the analyzed meteorological data and calculations required to derive the necessary radiation and evapotranspiration variables for the rtSHM are completed. SHM is then executed for each grid point in the model domain and produces simulated SW fields for the surface, root-zone layer and a deeper layer, required as part of the initial conditions for the rtMM5.

The process of executing the rtSHM has been automated to the point of requiring minimal operator assistance/time. The process described above has been executed for the period 8 May 1995 to the present, and it runs operationally every day, to update the SW fields for the previous 24-h period.

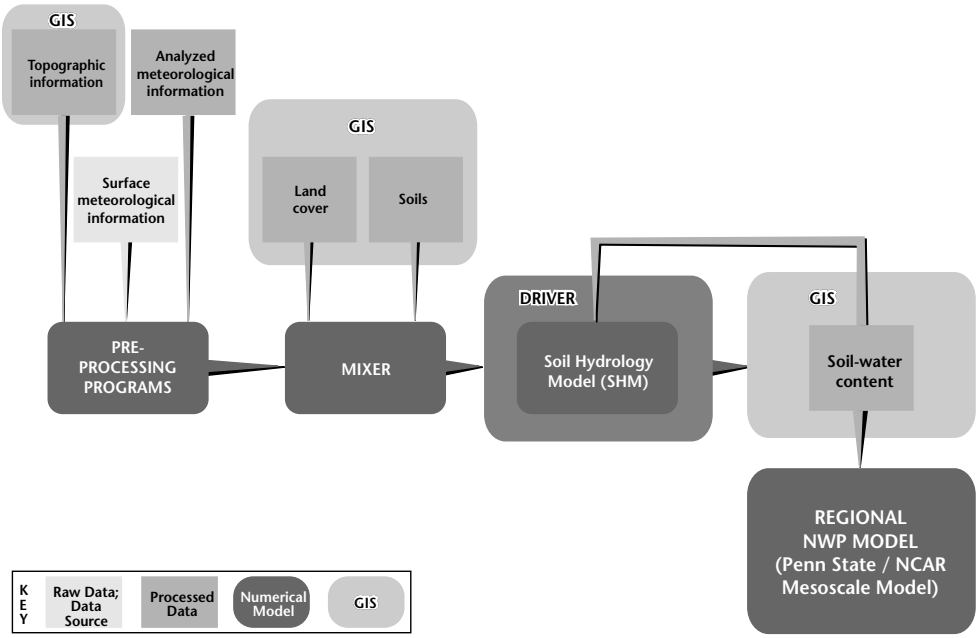

Figure 11: The real-time SHM system.

Precipitation is a critical SHM driving variable. As part of the PSU-MSFC collaboration of Lakhtakia and Goodman, MSFC provided a radar-derived precipitation product in early March 1996. This product consists of 6 hourly cumulative precipitation analyses, at 2-km resolution over the 48 contiguous United States (Figure 13). Software was developed to integrate this information into the precipitation-analysis procedure which is part of the pre-processing programs. This procedure is done in two steps: a first-guess analysis is created and then a Cressman-type of objective analysis is performed. When only the station observations are available, the first guess is created using the station observations and an interpolation. The NEXRAD-derived precipitation information has replaced this first step. The final precipitation analysis is a product of the blending of the radar and station information. In most cases, the use of this new source of precipitation has resulted in an improvement in the final 12 hourly precipitation analysis used by the rtSHM (Lakhtakia, 1997).

An example of this improvement is presented in Figure 14. The analyzed precipitation field (Figure 14a) was obtained using only the station observations shown in Figure 15, while Figure 14b shows the result of blending the radar product (Figure 13) with the surface observations. In this case, the radar-derived precipitation and the station observations indicate the existence of a narrow frontal band of precipitation located in the midwest and oriented in the southwest-northeast direction. When using only the station observations, the analyzed fields do not show the continuity of the precipitation band instead, the analysis consists of a series of disjoint precipitation areas. When using both sources of information, the resulting analysis looks more realistic.

The rtSHM and the rtMM5 require the specification of two types of land surface information: land cover and soil texture. The land cover information is derived from the 1 km United States Geological Survey—EROS Data Center (USGS-EDC) Land-Surface Characteristics Database (Loveland et al. 1991) (Figure 12). Until not long ago, the only source for the soil texture information for this type of application was the land cover information, which was converted into soil texture using a lookup table (CONV soil texture). Recently, the STATSGO-derived soil texture product (CONUS-SOIL) has become available. Therefore, testing is required to see what effect it has on the results of the rtSHM and rtMM5.

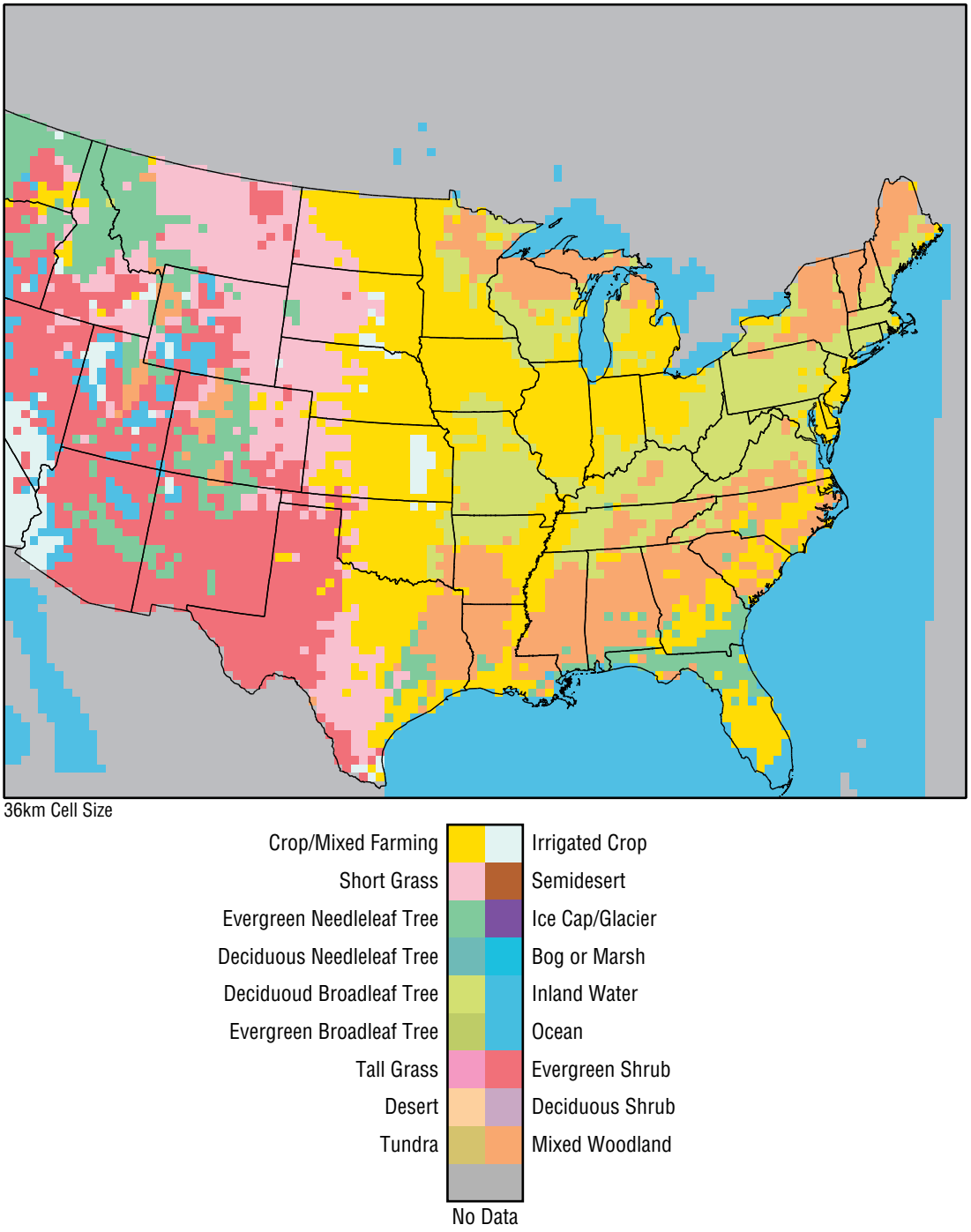

Figure 12: The rtSHM and rtMM5 geographic domain with the land-cover distribution.

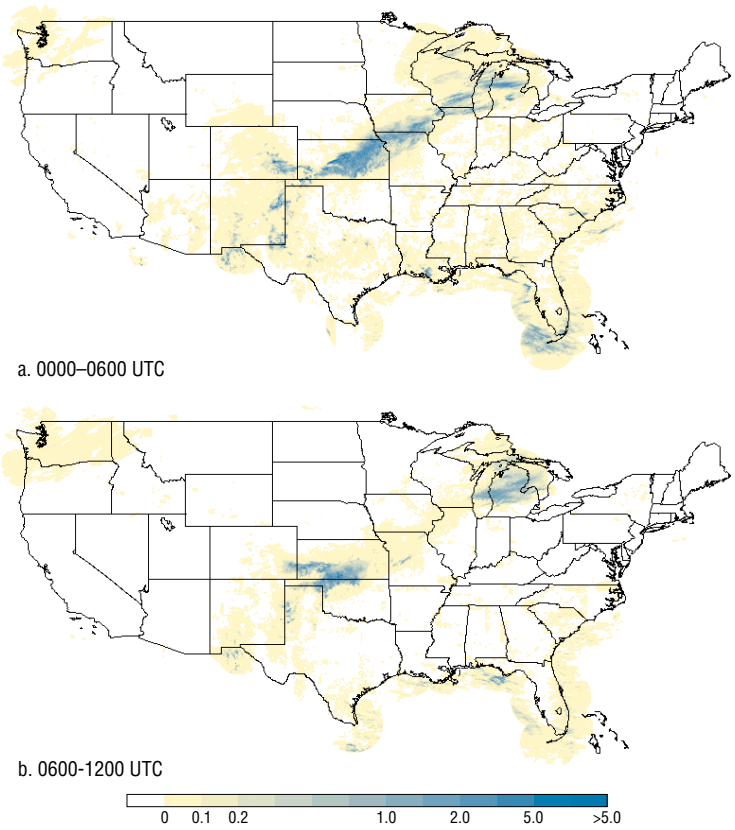

Figure 13: The NEXRAD-derived 6 hourly cumulative precipitation analysis (in inches) for the United States for the periods: (a) 0000-0600 UTC and (b) 0600-1200 UTC, 20 August 1996.

In order to test the link of the rtSHM and rtMM5 in a systematic manner, a series of different rtSHM and rtMM5 setups are used. There are two setups for the rtSHM, which make use of the two sources of soil texture: CONV and CONUS-SOIL. Five runs using the rtMM5 are made for selected days (Table 2).

In the noBATS setup, rtMM5 uses a simple representation of the surface processes and a climatological value of the soil moisture. This can be considered a "control setup" because it is a well tested model setup. In all the other cases BATS is used to represent the surface-atmosphere interactions within MM5. In the noSHM setups, MM5 uses climatological values of SW as initial conditions for the soil water variables, and both soil texture sources (CONV and CONUS-SOIL) for BATS. Finally, in the SHM setups, the rtMM5 is linked to the rtSHM, which provides daily updated values of SW.

The rationale for choosing a particular day for a set of rtMM5 simulations (numerical experiment) is that the northeastern US should have fairly clear skies, without precipitation, and with strong radiational heating. Under these circumstances, it is expected that the surface effects on the atmosphere are more important. As a result, it should be easier to study the effect of the changes in the surface characteristics, such as soil texture (i.e., CONV versus CONUS-SOIL), and SW source (i.e., climatology versus rtSHM) and the surface physical representation (i.e., no BATS versus BATS) on the afternoon air temperature and humidity in the lower atmosphere. All rtMM5 runs in the different numerical experiments are initialized at 0000 UTC, and extend for a period of 24-h.

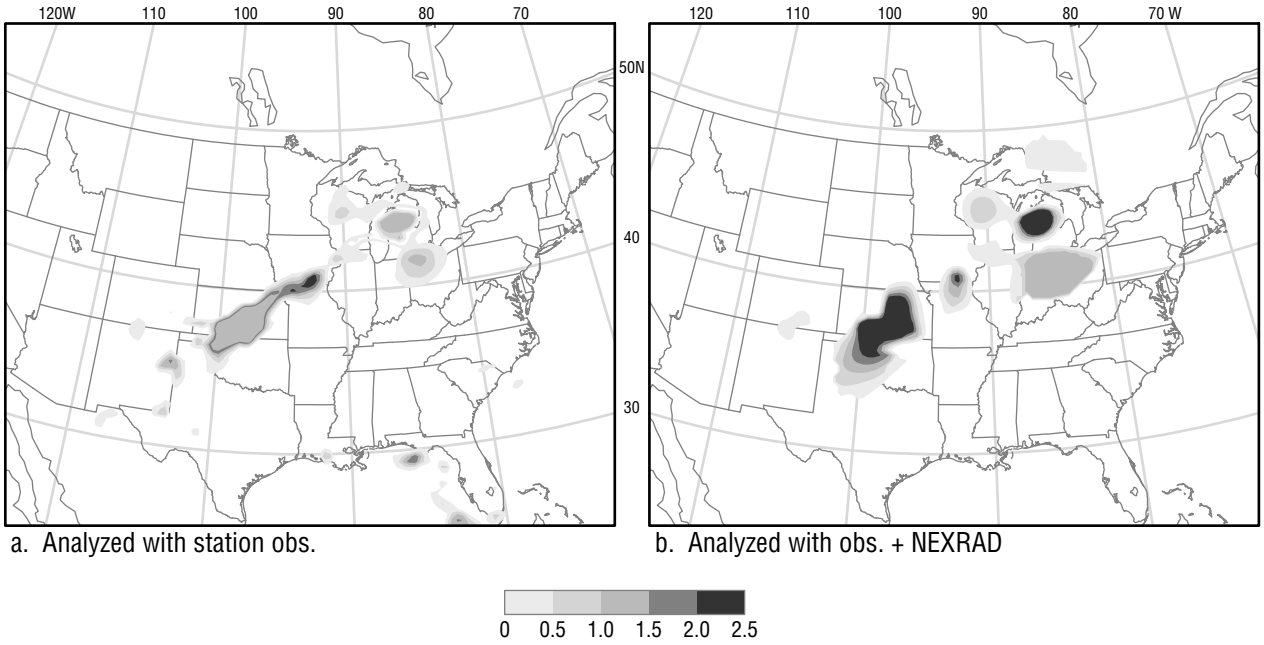

a. Analyzed with station obs.

b. Analyzed with obs. + NEXRAD

Figure 14: The analyzed 12 hourly cumulative precipitation (cm) for the period 0000-1200 UTC, 20 August 1996, obtained using: (a) station observations and (b) NEXRAD-derived analyses and station observations

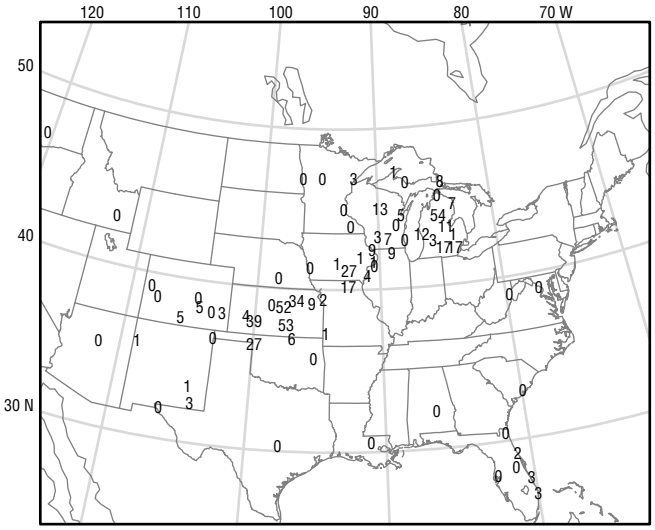

Figure 15: The observed 12 hourly cumulative precipitation (mm) for the period 0000-1200 UTC, 20 August 1996

	rtMM5	BATS	SHM	SoilTexture
1.	noBATS	no	no	no
2.	BATS_noSHM-CONV	yes	no	CONV
3.	BATS_noSHM_CONUS-SOIL	yes	no	CONUS-SOIL
4.	BATS_SHM_CONV	yes	yes	CONV
5.	BATS_SHM_CONUS-SOIL	yes	yes	CONUS-SOIL

Table 2: Summary of model runs testing the impact of different land cover and soil texture inputs

As an example, the numerical experiment initialized at 0000 UTC on 19 August 1996 is discussed here briefly. Figure 16 shows the SW for the root-zone layer, simulated by the rtSHM, for both types of soil texture. These are the fields used in the initialization of the rtMM5 when linked to the rtSHM (i.e., BATS_SHM_CONV and BATS_SHM_CONUS-SOIL). When comparing these two fields, the most noticeable features are the lower values of SW, and the higher horizontal variability of SW, when using the CONUS-SOIL soil texture. CONUS-SOIL has been developed only for the US. Therefore, there is no difference in the fields in Canada and Mexico because CONV soil texture was used in these areas.

The 1996 Summer season has been fairly moist in the northeast United States and fairly dry in the southwest (e.g., Texas). The status of the soil is exemplified by the Drought Severity Index for the week of 17 August 1996 shown in Figure 17. In general terms, this compares fairly well with the SW fields shown in Figure 16.

Figure 18 shows the analyzed air temperature (T) observations, and the simulated T from the different rtMM5 runs, at the lowest model level (close to the surface), 24 hours into the simulations (i.e., at 0000 UTC on 20 August 1996). In general, all the simulations [Figure 18b–f] produced stronger temperature gradients when compared to the observations [Figure 18a]. In particular, the simulations using the linked rtSHM and rtMM5 (i.e., BATS_SHM_CONV [Figure 18d] and BATS_SHM_CONUS-SOIL [Figure 18f]) show even stronger gradients. Focusing on Pennsylvania, the linked simulations show higher temperatures than observed, and even higher with SHM than those simulated with rtMM5 using climatological values of the SW (i.e., the first 3 setups shown in Table 2). It is interesting to note that MM5 attempts to create a frontal boundary which runs from the Great Lakes to the southwestern states (Figure 18b). Inclusion of BATS enhances this frontal boundary (Figures 18c and 18e), which is further sharpened when the SHM-simulated SW is used (Figures 18d and 18f). The analyzed temperature reveals a weak frontal boundary (Figure 18a).

These results are preliminary. In particular, it should be noted that many numerical experiments should be performed, and the results analyzed, in order to have a clear idea of the effect of the use of BATS within MM5, and of the effect of the rtSHM and rtMM5 link. This validation will constitute the main focus of attention during the coming months. At least two journal publications are expected to result from this work.

SHM Snow Component

(B. Capehart—PSU)

The soil hydrology model is being modified to include the Utah Energy Balance Snow Accumulation and Melt Model (UEB) (Tarboton and Luce, 1996). UEB is designed to run with minimum meteorological data and shares several parameters with SHM. UEB can be run within the SHM environment for as long as it calculates the presence of a snow pack. Initial tests of the SHM-UEB model indicate some sensitivity to snow cover in the winter months (when the soil is at or near saturation). However, there is little sensitivity to the inclusion of the snow component for the summer months (when the soil water content varies the most, and therefore, where SHM would be most useful). Further development, tests and validation of SHM-UEB are in progress.

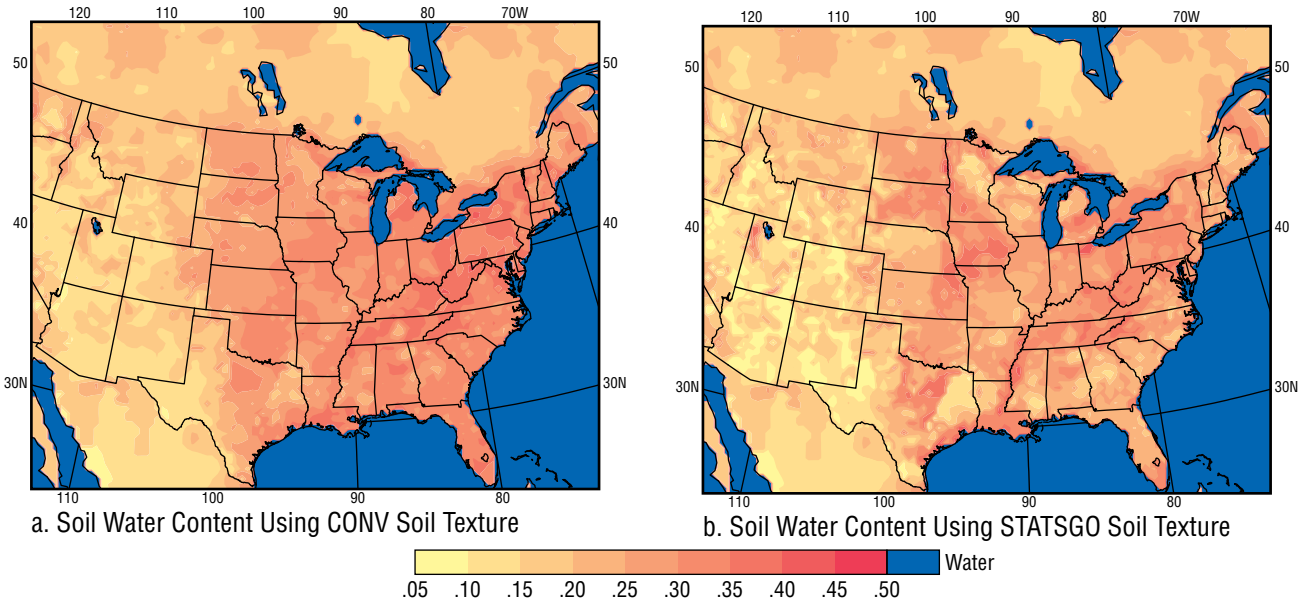

Figure 16: Soil water content simulated by the rtSHM for 19 August 1996 for (a) CONV soil texture and b. STATSGO soil texture.

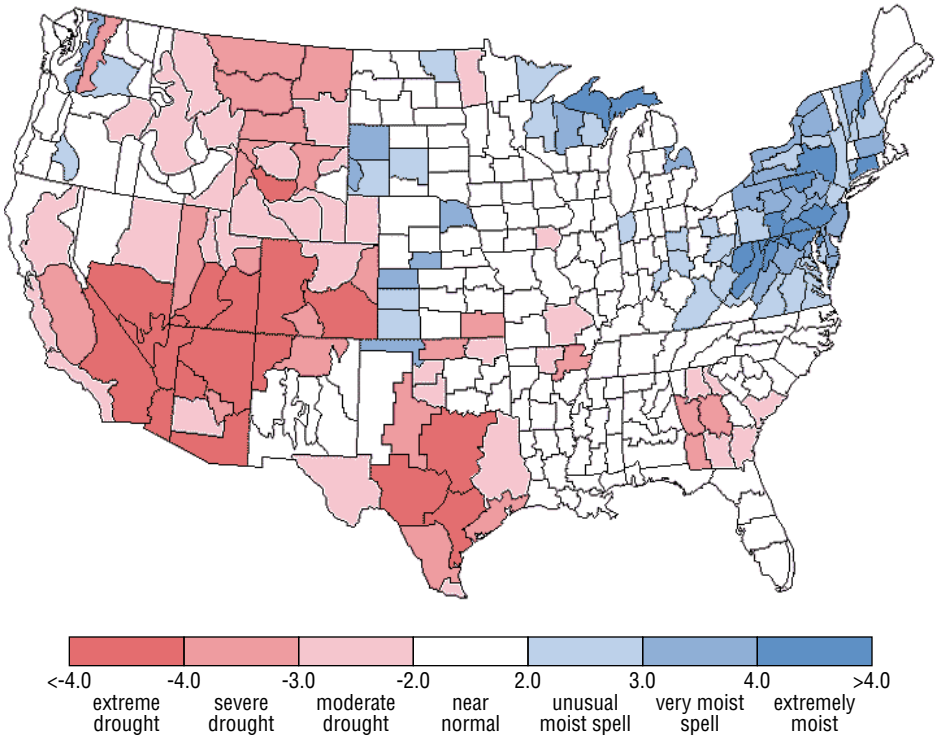

Figure 17: The Drought Severity Index for the United States for 17 August 1996.(Source: the Climate Prediction Center, NOAA, World Wide Web site).

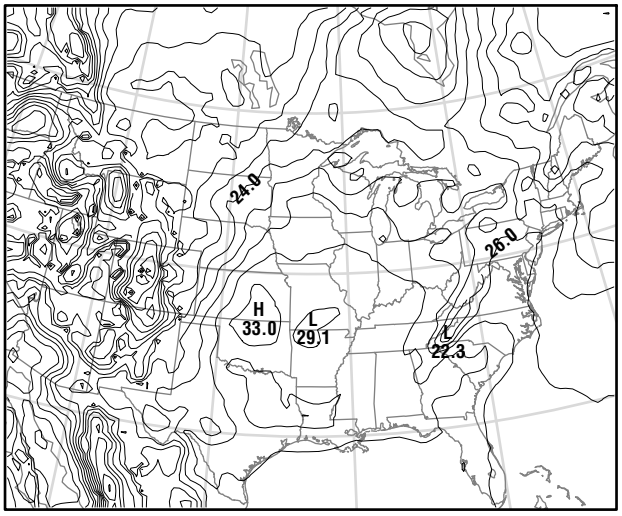

a. Analyzed

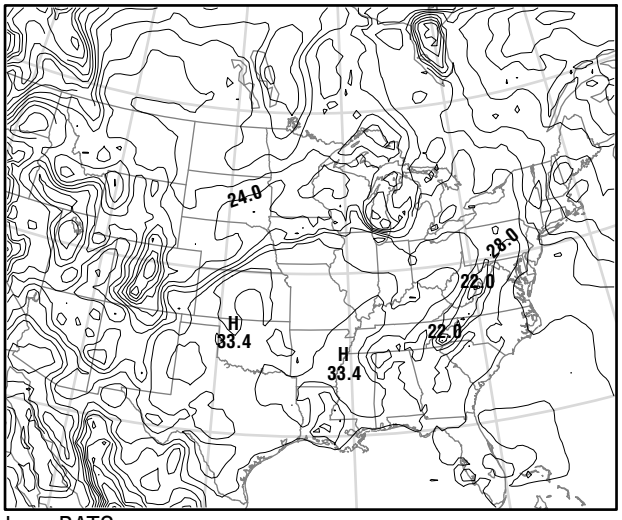

b. noBATS

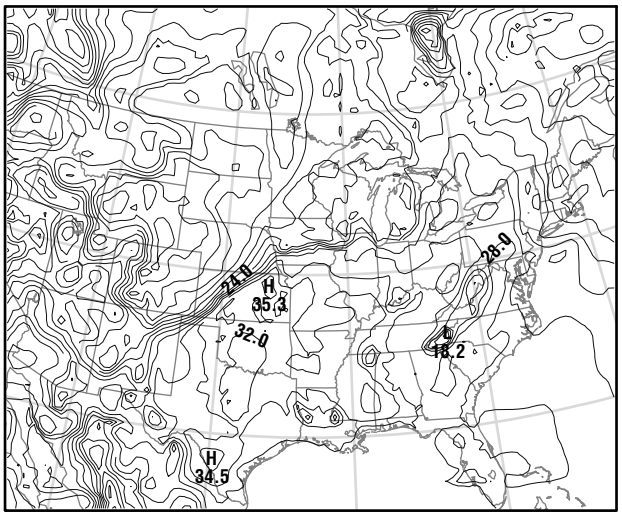

c. BATS-noSHM-CONV

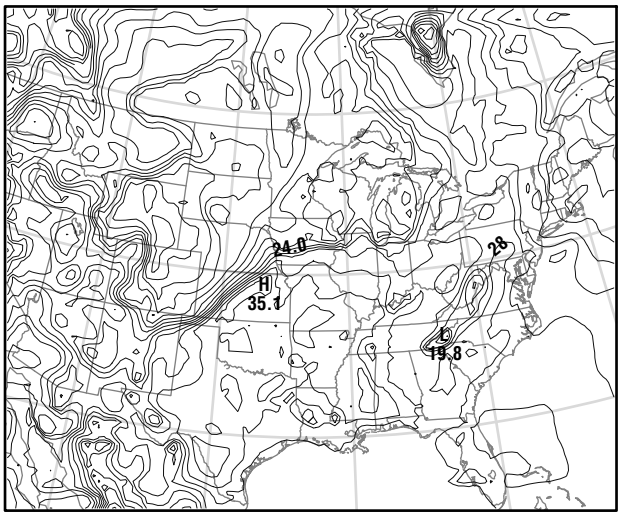

d. BATS-SHM-CONV

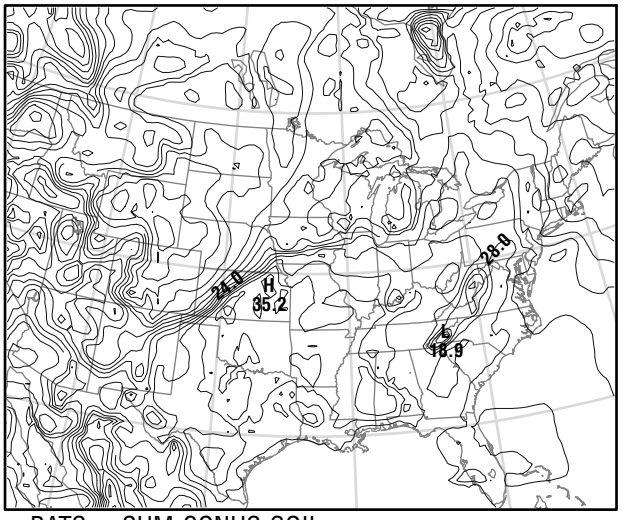

e. BATS-noSHM-CONUS-SOIL

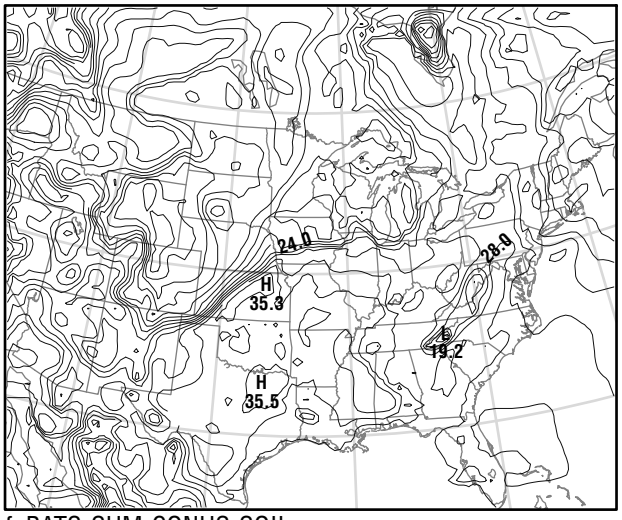

f. BATS-SHM-CONUS-SOIL

Figure 18: a. Analyzed and b–f. simulated temperature (C) for 0000 UTC 20 August 1996. The simulations were performed using the following rtMM5 setups: (b) noBATS; (c) BATS-noSHM-CONV; (d) BATS-SHM-CONV; (e) BATS-noSHM-CONUS-SOIL; (f) BATS-SHM-CONUS-SOIL

Storm Simulations

(B. Yarnal, M. Lakhtakia, D. Johnson, B. Frakes, E. Beighly, R.A. White, D.A. Miller—PSU)

Linked MM and Terrestrial Hydrology Model (THM) Simulation

The linkage of the SHM, the MM, the THM, and the WQM is central to the SRBEX effort (Figure 4). It consists of the SHM providing the initial soil water content to MM5, MM5 providing simulated precipitation data over the SRB to the THM, and the THM providing the hydrographs at various points throughout the basin to the WQM, which then uses them to predict the chemical nature and reactivity of the runoff.

In order to perform a first test of the linked-model strategy and to identify bottlenecks in the transfer of data from one model to another, we chose a single storm event subject to the following criteria: (1) Near, but not over bank-full discharge on a regionally extensive set of gages. This gives a good volume of water without the complications of over bank flooding on a regional extensive storm. (2) No snow on the ground or in the storm. We did not want the complication of snow melt in the model. (3) Leaf off conditions. We did not want to have the added complication of dealing with transpiration in the THM at this early stage. A search of the relevant hydrologic and meteorologic records produced 10 possible storms. As a second step, we needed to determine which of these strong hydrographic responses would be best to model. The working assumption was that the MM would be more effective modeling precipitation from a typical storm. Similarly, it was assumed that the THM could reproduce the hydrographic trace generated by an archetypal storm's precipitation. Thus, of the storms associated with the high-discharge events, which one was most representative? Synoptic climatology was used to answer this question. These results suggested that it should be possible to determine subjectively the most representative event by studying the weather maps and storm trajectories associated with the strong hydrographic responses at WE–38, an experimental watershed in east central Pennsylvania. The analysis indicated that the 9 April 1986 storm was clearly the best choice, possessing a well-defined, normal evolutionary sequence for wave cyclones.

Once the 9 April 1986 storm event was identified as the best choice for our first linked-model experiment, the third step was to define the MM nested domains for this simulation. The MM used a set of three nested domains with grid cell sizes of 36, 12, and 4-km. Grid dimensions are 70 rows by 70 columns, 108 by 114, and 108 by 108, respectively. The 4-km domain is centered on the SRB. Since most storm events approach the SRB from the west or south, the 12 and 36-km domains both extend considerably further to the west and south of the SRB than to the east and north. The remaining MM5 initial and boundary conditions were then created from observations and a 48-hour simulation was performed. The MM5-simulated precipitation fields were output on an hourly basis. Since the MM5 simulation was performed on the CRAY-YMP, we had to develop software to read the precipitation output and gather the required information from the MM run, transfer it to the ESSC SUN workstation network, and convert it to a GIS-compatible format. Standard GIS tools were then used to regrid the precipitation fields for use by the THM as a forcing term in the surface hydrology balance (Lakhtakia et al., 1996).

The MM5 simulation captures the spatial and temporal structure of the storm event, while THM represents the timing of the event well. The Curve Number method generates a somewhat realistic hydrograph with both analyzed and simulated precipitation, and a minor adjustment can further improve the basin response using this approach. In contrast, the hydrographic response generated by the Green-Ampt equation is inferior. Several related factors contribute to these poor results, including: the nature of the precipitation event chosen for the experiment; the inability of MM5 to simulate small, high-intensity precipitation cells embedded in the widespread, moderate precipitation; and the influence of the two dominant surface soil-texture classes on infiltration rates.

Ongoing And Future Storm Simulation and Scaling Issues Research

An important goal of the research is to develop a modeling system that can accurately project basin runoff on seasonal to interannual time scales. To reach this goal, THM and MM5 will need to be modified considerably and several intermediate model experiments will need to be run.

Although the current version of THM has a state-of-the-art surface routing scheme, the model has several deficiencies. Its single biggest drawback is its lack of a subsurface component. Adding to this problem, THM's infiltration scheme cannot handle more than one storm. However, adding a subsurface flow model is a difficult proposition because most operate on relatively small basins with fine time steps, while those that work on larger spatial and temporal scales are so highly parameterized that they are more empirical than physically-based. Nevertheless, work has started to link the surface routing scheme of THM to a physically-based component explicitly aimed at simulating the subsurface flow of larger basins at monthly to interannual time scales.

At the same time that the above changes to THM are taking place, the following modifications will be made to MM5:

- The resolution of the planetary boundary layer scheme will be decreased to make the routine more appropriate for monthly to interannual time scales and to improve performance.
- The model will be optimized for multitasking.
- The model will be altered to receive GCM data.

Although none of the changes to MM5 are conceptually difficult, they are time consuming.

While the above model development of THM and MM5 is underway, two sets of sensitivity analyses are being run using the current versions of THM and MM5. The first set compares four spring storms: the April 1986 storm described in detail above (Yarnal et al., 1997), and storms from May 1984, June 1982, and May 1988. For each storm, both analyzed and MM5-simulated precipitation is being used to drive THM. The objective of these model runs is to confirm the positive results obtained from the April 1986 storm experiment, to test model sensitivity to antecedent moisture conditions, and to explore the sensitivity of the results to various storm trajectories and configurations.

Also, from this round of model runs, the research team will select the "best" storm to use in the subsequent experiment. In that second sensitivity analysis, THM will be driven by the precipitation produced by fully nested (36, 12, and 4-km), partially nested (36 and 12-km, and 36 and 4-km), and unnested (36-km) runs of MM5. The objective is to determine the effect of nesting on the linked model system; these results could simplify and speed up subsequent experiments considerably.

After these sensitivity analyses are run and the THM and MM5 model development is completed, the following staged experiments will take place:

1. Multistorm simulation. This experiment will be the first to use the modified THM (physically-based, with linked surface and subsurface routing schemes) and MM5 (multitasked, optimized, and with the new radiation and PBL schemes).
2. Annual cycle simulation. Next, the annual cycle will be modeled, accounting for changing base flows and snow melt, as well as individual storms.
3. ENSO event simulation. Finally, an ENSO cycle from the AMIP period will be simulated. This experiment will involve two separate runs. The first will simulate the event using global, regional, and local observations. The second will use GCM output for the large-scale (global and, perhaps, regional) inputs.

The ultimate aim of this evolutionary process is to use ENSO GCM forecasts to predict basin runoff up to 18 months in advance. The difference between this research and similar projects is that while others essentially use simple water-balance approaches for large basins, the SRBEX linked-model approach will explicitly model the evolving hydrology on a storm-by-storm basis. The output from this system will provide the fine spatiotemporal resolution required by many decision makers who manage or depend on water resources.

Soil-Vegetation-Atmosphere Transfer Modeling and Remote Sensing

(T. Carlson, D.A.J. Ripley)

Introduction

We have completed an investigation of urbanization in the State College area and have begun work on two additional target sites: Chester Co., Pennsylvania, and Costa Rica. State College served as a test area for developing our methodology: the target area is small and lightly populated, but it is undergoing rapid urbanization. Chester Co., is much larger and riddled with urban centers, some of which are undergoing rapid development—mostly at the expense of farmland; (Table 3). Costa Rica is undergoing both a very high rate of urbanization around its principal city, San José, and had been experiencing a very large overall rate of deforestation (about 4% a year) until a decline began a few years ago.

Surface Type	1987	1988	1991	1993	1996
Agriculture	71.8	70.8	69.3	67.5	66.0
Forest	16.8	16.9	15.1	14.7	14.7
Developed	10.9	11.6	15.1	16.3	19.0
Water	0.5	0.6	0.45	0.38	0.3
Cloud, etc.	0.01	0.15	0.0	1.02	0.0

Table 3: Percentage Classified for Each Category, Chester Co.

The purpose of the investigation is to use a new method for deriving land surface parameters from a combination of thermal infrared and vegetation index measurements obtained by satellite (Landsat-TM and NOAA-AVHRR) and to integrate these parameters with more conventional data bases. Our intent is to show that it is possible not only to monitor land use changes over time by satellite with conventional descriptors (percent developed, agriculture, forest, water) but to express these same land use change in terms of physically-based surface climate variables derived from the satellite measurements—moisture availability (Mo) and fractional vegetation cover (Fr). By physically-based we mean that the surface energy fluxes can be calculated from these two parameters, which are the dominant ones governing the surface energy budget in land surface models. Moreover, given a field of Mo and Fr and a specific urbanization or deforestation scenario, future changes in local microclimate can be made with the aid of an atmospheric mesoscale model.

Present Investigation

A Review of Results from the State College Study

A major effort in our research has been devoted to the study of urbanization using the so-called triangle method (Gillies and Carlson, 1995). In the first phase, Owen (1995); see also Owen *et al*. (submitted), completed an analysis of the State College, PA, area in which values of Fr and Mo were determined from AVHRR data over a 30x30 km domain. The object was to see if the migration of pixels within the Fr/Mo space (the triangle) were coherent and could be related to the nature and extent of urbanization. Eight AVHRR scenes were obtained (two per summer every other year) between 1986 and 1994. Additional Landsat TM scenes were obtained, from which percent urban development was calculated and classified as to forest, agriculture, developed and water.

Results, summarized in Owen *et al*. (submitted) and Carlson and Owen (1996), are that (1) AVHRR data can detect neighborhood-scale changes in urbanization, (2) Mo seems to constitute an intrinsic descriptor of the surface fabric, in addition to being a fundamental land surface parameter which governs local microclimate, (3) changes in Fr and a scaled infrared surface radiant temperature (T^*_r) (as well as evapotranspiration) accompany significant changes in urbanization. Mo, however, does not appear to change significantly with increasing urbanization, at least when agricultural land is developed. Fr decreased substantially from the summer of 1985 to the notoriously dry summer of 1988 (but recovered in 1991), whereas Mo hardly changed during that period. (4) tree cover appears to be a dominant mitigating factor in the aforementioned changes in land surface parameters. Tree cover seems to affect Mo.

Chester County Study

Following our methods developed for State College, analyses have begun of images for Chester County, PA. Chester Co., located just west of Philadelphia, is about four times the area of the State College target area. Parts of the county are undergoing rapid urbanization.

AVHRR scenes from 1986 to 1995 have been converted to temperature and radiance values, corrected for atmospheric attenuation and georeferenced; this has also been done for a fewer number of Landsat TM scenes covering roughly the same period. Initially, the procedures parallel those applied to the State College images. As in the case of State College, summer scenes are used because they are subject to the least variability due to changing meteorological conditions, and because summer scenes permit a better distinction between forest, agriculture and developed land than spring or winter scenes. From these image data, we determine Mo and Fr and then relate these parameters to the conventional land use categories as they evolve over the previous decade.

All TM images have been classified according to several basic land surface types. Although the latter operation involves designating a variety of types, the final analysis consolidates all classes into four categories: developed, forest, agriculture (including pasture and bare land) and water. A summary of these four classes by percent is listed below in Table 3. The table shows a progressive increase in developed land, which occurred largely at the expense of farmland. Unlike the corresponding values for State College, forested area in Chester Co. underwent a small but non-trivial decline. Much of this decrease in forested area pertains to the loss of trees in and around new developments, rather than the loss of land formally designated as forest. Instead, new housing in wooded areas in at least partly responsible for the decline in the forest category.

To verify these statistics, several approaches have been taken. The first was to compare our designated categories with those determined by aircraft and in situ methods, as published by the Chester Co. planning office in West Chester, PA (courtesy of Mr. Wayne Clapp). The published classification for 1987 was compared with our 1987 classification based on the Landsat image. We then determined a verification matrix from which we calculated user accuracy and producer accuracy (Congalton, 1991). These results are shown in Table 4.

Surface Type	User Accuracy	Producer Accuracy
Veg/Crops	76	96
Forest	87	75
Developed	93	54
Water	100	100

Table 4. User and Producer Accuracy: Chester Co. (1987 Survey)

User accuracy is calculated by dividing the number of correctly classified pixels in a land cover category by the total number of pixels classified in that particular category. This statistic represents the probability that a pixel classified using remotely sensed data actually represents that class. The producer's accuracy is calculated by dividing the number of correctly classified pixels in a land cover category by the total sum of that category. This represents the probability that a reference pixel is correctly classified.

For example, the producer of the 1987 classified image can claim only that 54% of the time an area that was actually developed was identified as such. However, a user of the classification map will find that if they were to visit a site that the map indicates is developed, 93% of the time it will have been developed.

A second method, which is based on determining the so-called the KHAT statistic (Congalton, 1991), involves not only the correctly classified pixels but the off-diagonal elements in the matrix. KHAT takes into consideration confusion among classes. For the 1987 image, the result is a KHAT of 81%, which implies that the classification process avoided about 4/5 of the errors that a completely random classification would generate. This result is in agreement with other remotely derived land cover classifications (Tin-Seong, 1995).

Producer accuracy tends to be lower for developed areas than non-developed areas because of confusion between medium density buildings and bare soil. Tin-Seong (1995) found that this ambiguity accounted for about one-third of the error. In our 1987 image, developed areas were predominantly misclassified as either vegetated grassy field or forests. Spectral confusion of land cover types is aggravated by the spatial heterogeneity and mixed pixels typical of urban settings. Developed areas tend to include a considerable interpixel and intrapixel variation which is found less over forests or water bodies. Above all, a distinction must be made between spectral and societal classifications. Both may be correct within their own context.

Additional significance testing for the Landsat classification when combined in 1 km squares in order to assess the confidence in determining the percentage of developed area. Classified Landsat TM images were subset into 1-km squares (roughly comparable to the resolution of the AVHRR), each containing 1600 pixels assigned to one of the five categories listed in Table 2. From this arrangement, a 2x2 matrix was created for each of the 1-km pixels for two images at two different years; this is shown in Table 5.

	Time 2	Time 2
Time 1	**Developed**	**Not Developed**
Developed	X_{11}	X_{12}
Not Developed	X_{21}	X_{22}

Table 5. Matrix for obtaining p-value for development assessment

The diagonal elements represent pixels which have experienced no change in classification between the two times in question. Off-diagonal elements represent pixels which have changed from either undeveloped to developed or vice versa. A null hypothesis of no change over time is equivalent to a hypothesis of symmetry in the matrix. No development in time requires that the off-diagonals must be either zero or that $X_{12} = X_{21}$, which is to say that as many pixels changed from undeveloped to developed as from developed to undeveloped.

Following Eliasziw's (1991) McNemar test for a 2x2 table, we are testing the null hypothesis of marginal symmetry by calculating the p-value: $(p(\chi_1^2 \geq z^2)$, where:

$$z^2 = \frac{(X_{12} - X_{21})^2}{(x_{12} + x_{21})}$$

The p-value is determined by comparing the z^2 value to a chi-square distribution density function with one degree of freedom, which yields the probability of obtaining a χ^2 greater than or equal to the calculated z^2 value. A low probability indicates strong evidence that the off-diagonals are not symmetric and there has been a significant change in land use over time.

Qualitatively, at least, the general development trend demonstrated by classified Landsat TM images reflect the changes which have been reported for Chester Co. by the Chester Co. Planning Commission. These patterns of change, shown by the classified TM images for 1987 and 1996 (Figures 19 and 20) reflect continued suburban expansion outward from Philadelphia (denoted by the letter 'a' in Figures 19 and 20) into eastern Chester Co., as well as the development of 'bedroom communities' out of Delaware (location 'e' in Figures 19 and 20). At a first glance, we are likewise finding the most development between 1987 and 1996 in the West Chester borough and the surrounding townships along route US 202 in the east and along US 30 which runs through the middle of Chester Valley (location 's' in Figures 19 and 20).

Present development, as revealed by Landsat, presage the Planning Commission's projected development trends for the year 2000, in which the eastern part of the county along US 30 becomes densely development and the previously distinct centers of development become more of a continuous mass stretching through the eastern half of the county. Although major roads serve as conduits for rapid and dense urbanization, many tiny, isolated pockets of development are already starting to form in the highly rural southwestern part of the county (location 't' in Figures 19 and 20). These areas are projected to increase in size and number.

The decrease in forest from 1987 to 1993 reflects this development pattern, as most of the land use change occurred along the US 30-202 axes. In the classification, the highly wooded residential areas of this region often appear as grids of forest and developed classes. With continual expansion of the urban fringe out of Philadelphia, the developed class expanded significantly in 1996, resulting in a loss of forest class. No loss in forest was detected between 1993 and the present.

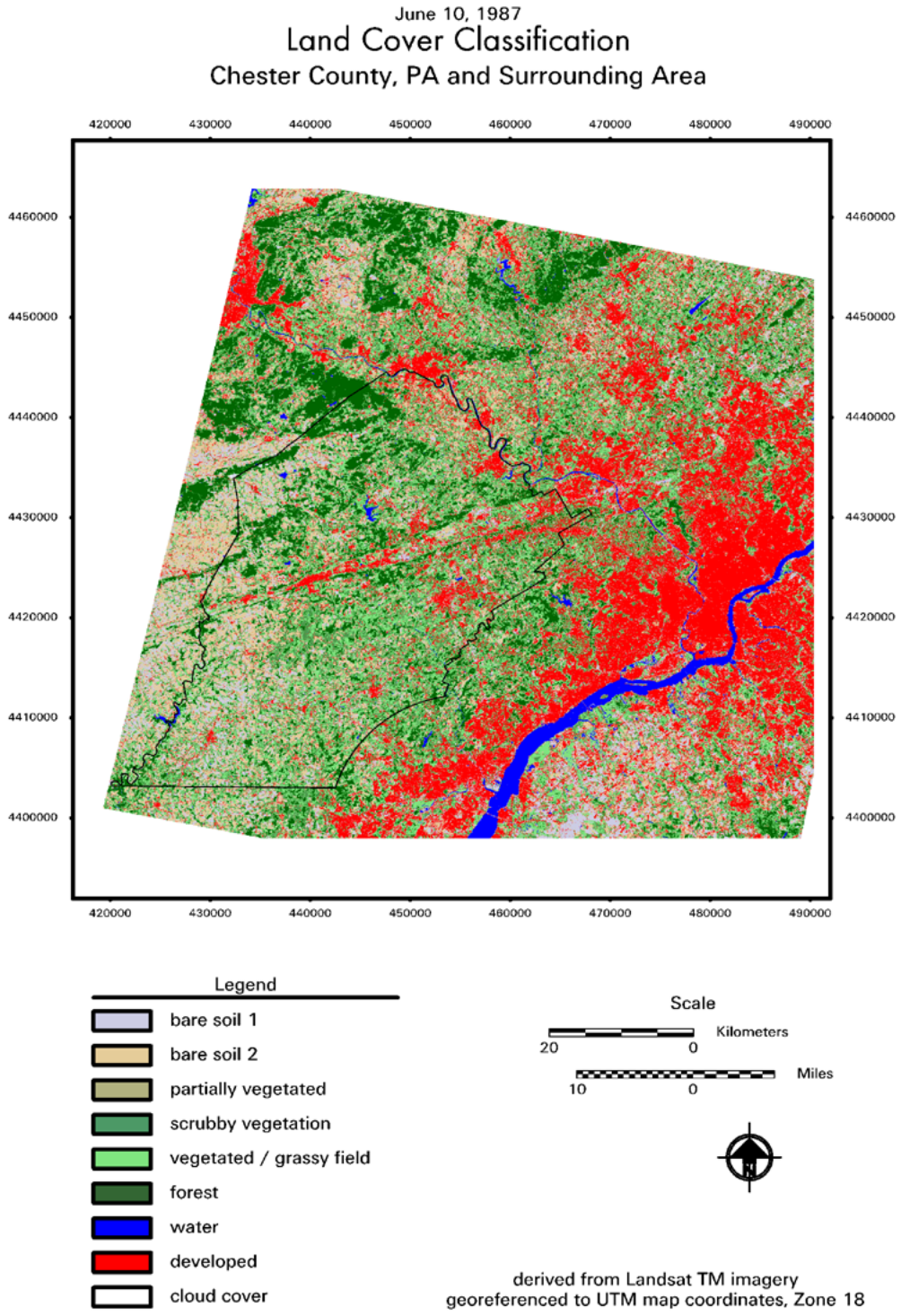

Figure 19. Classified Landsat TM image for June 10, 1987 over Chester Co. Letters denote locations referred to in the text. The outline of Chester Co. is shown by a thin solid border in the background. Categories referred to in the text (Tables 4 and 5) correspond to those in the legend except that the agricultural classification includes the five bare soil and vegetation classes.

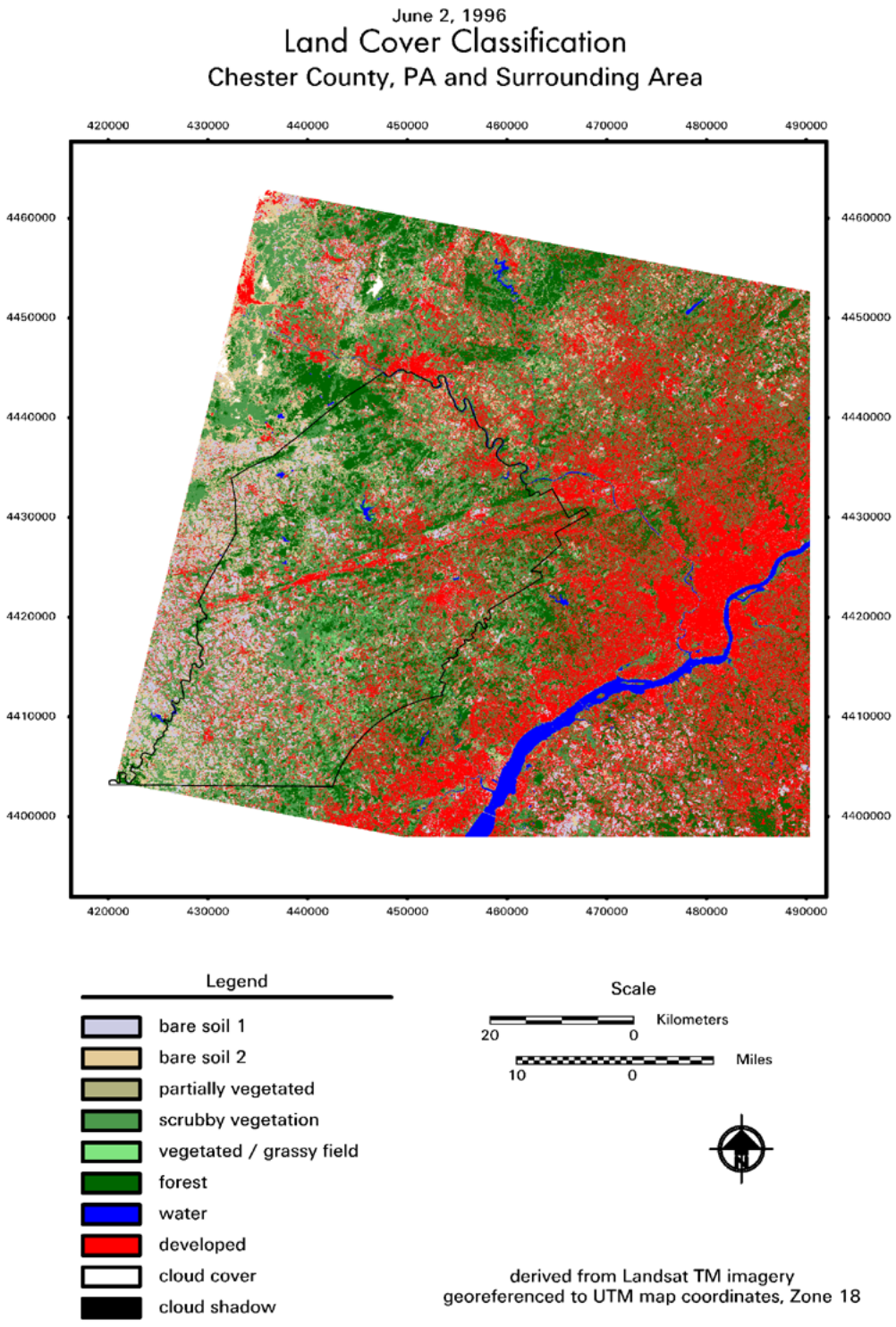

Figure 20. Same as Figure 19 except for 2 June, 1996.

We have also attempted to compare the 1996 classification with observations made in the field. In September, we conducted a field survey of Chester Co. during which time we were able to locate (using a Trimble™ GPS) about 50 pixels in the Landsat image and to classify the locations visually.These measurements were made on two occasions during September and October, 1996. Statistics are summarized in Table 6.

Surface⇒ Satellite⇓	Vegetation Agriculture	Bare Land Agriculture	Forest	Water	Developed	Row Total
Vegetation Agriculture	10	0	1	0	5	16
Bare Soil Agriculture	3	6	2	2	0	13
Forest	0	0	3	0	1	4
Water	0	0	0	1	0	1
Developed	0	0	0	0	15	15
Column Total	13	6	6	3	21	49

Table 6. Accuracy assessment for GPS field measurements; numbers of observations;

Overall accuracy was 71.4%.The off-diagonals of the error matrix were due to definable and repeated misclassification, particularly of large, uniform corn fields as bare land/agriculture. Errors are most likely due to the difference in dates between that of the satellite image and the field measurement, to errors in the GPS instrument (about 30 m), and to errors in georegistration. More surface information is needed to clarify these errors; further ground truth measurements may be made in the Spring of 1997.Additional error may have come from some cloud contamination which caused the image to be slightly fuzzy in places.These errors tended to show up as the misclassification of pixels as agricultural or bare ground.

One significant cause of error highlights a fundamental uncertainty in classifying urban areas; this is a tendency to overclassify residential areas as forest or agricultural land. Many of the suburban areas showed up as wooded or as agricultural when they were actually landscaped residential developments. However, in each case the classified image clearly discerned the development in the region, appearing as gridded or splotchy patterns of vegetated/developed pixels. In general, developed pixels were found in the classified image within 50 meters of the misclassified pixel.This raises the important issue of accuracy in georeferencing the pixels. Classified images were georeferenced with a total RMS error of about 2.5 pixels (about 75 m)—a value within the limitations of map accuracy. Combined with the 30 m uncertainty in the GPS measurement, incorrect classifications were explainable by the limitations of map and GPS measurement.

In general, however, the Landsat classification provides a highly representative source for land use data in the region. Glaring misclassifications were very rare and many specific patterns, such as roads crossing fields were discernible. Large-scale agricultural and developed communities which were obvious in aerial photographs were clearly identified in the classified image.

AVHRR imagery is now being resampled and superimposed on the 1 km squares used to create the z^2 statistics (Table 5). Preliminary results which show that (1) neighborhood scale changes, referred to above, can be detected by AVHRR when changes in developed area is greater than 10%; (2) vegetation, notably tree cover, affects Mo more than individual precipitation events or

protracted dry or wet periods; Mo appears to be an intrinsic descriptor of land surface; (3) Mo responded very little to changes in development for a given type of development; (4) fractional vegetation cover and scaled surface radiant temperature changed significantly in response to urbanization; (5) evapotranspiration decreases at approximately the same rate as the increase in developed surface area.

At present, Chester Co. images are begin transformed to values of Mo, Fr and evapotranspiration. Their values at fixed UTM locations will be charted at selected locations over the past 10 years. As in the accompanying paper by Carlson and Owen (1996), pixel migrations will be followed within the context of the triangle. We plan to obtain additional land use and other socioeconomic data from the Chester Co. planning office. Scatterplots and analyses of Mo, Fr and evapotranspiration should be finished by early 1997.

Costa Rica

An allied project involves studying deforestation in Costa Rica. Deforestation has been considerable in this country during the past 30 years. Initially, our approach will follow procedures developed for Chester Co. Unlike Chester Co and State College, land use changes have come largely at the expense of forest land, rather than agriculture. A new and vital element in our Costa Rican program is a collaboration with Professor Arturo Sanchez (currently at the University of Costa Rica), who has acquired and georeferenced a number of Landsat TM images. Professor Sanchez brings to the project a considerable knowledge of the forest resources, ecology, hydrology and demographics of Costa Rica, as well as expertise in image processing and analysis. He has already prepared several extensive data bases for Costa Rica.

To the data set provided by Dr. Sanchez, we have added 5 more Landsat images and six AVHRR images over a 10 year period, 1986–1996. AVHRR scenes will be georeferenced to the Landsat images which have been rectified by Dr. Sanchez. A few more images for 1995 and 1996 may be collected before the end of the project.

The study centers on the capital area, San José and its surroundings, where the major effects on the forest and the countryside have occurred. Not all images are usable because of extensive cloud contamination, although all dates correspond to the dry season, which extends from December through March.

Georeferencing of TM and AVHRR images is being performed at the University of Costa Rica by Dr. Sanchez. Like our Chester Co. project, analyses will be made within the context of the triangle and the results related to socioeconomic and ecological changes. In regard to the latter, we will attempt to use the changes in Mo, Fr and evapotranspiration to describe how the deforestation exerts pressures on the boundaries of 'life zone' (regions of uniform ecology) in Costa Rica. This part of the project will be outlined in more detail in a later report.

Operational Goals

Not only does scaling allow us to compare pixel values from differing images, but it greatly minimizes errors due to atmospheric correction, instrument drift and viewing angle and therefore reduces the importance of obtaining absolute accuracy in deriving the surface parameters. Indeed, preliminary results using radiative transfer model simulations (Carlson and Ripley, in prep.) shows that scaling NDVI and surface radiant temperature yields almost identical values of fractional vegetation cover and surface moisture availability as would be obtained from radiances corrected with MODTRAN, a recent variant of LOWTRAN (Kneizys *et al.*, 1988).

This is illustrated in Figure 21, which shows scaled NDVI (N^*) based on the uncorrected (at sensor; $N^{*2}(a)$) and corrected (at surface; $N^{*2}(c)$) radiances. The figure not only confirms two

earlier and independent validations of a square root law between scaled NDVI and fractional vegetation cover (Choudhury et al., 1994' Gillies and Carlson, 1995), but suggests that the relationship holds equally well for uncorrected as for corrected radiances.

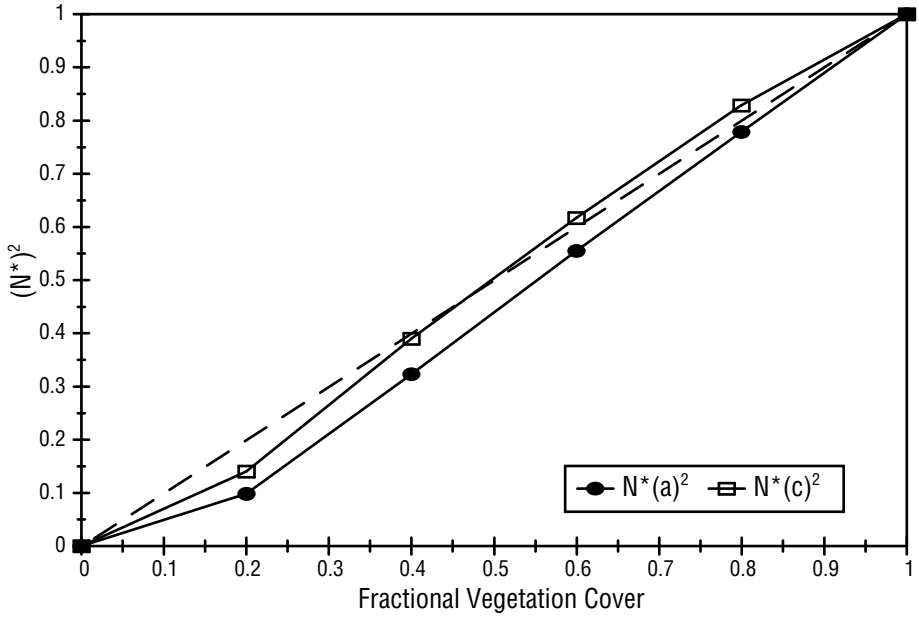

Figure 21. Simulations with a simple radiative transfer model for scaled NDVI squared (N^{*2}) versus fractional vegetation cover (Fr) based on the uncorrected (at sensor; $N^{*2}(a)$) and corrected (at surface; $N^{*2}(c)$) radiances. The solid sloping line without symbols represents a 1:1 correspondence between N^{*2} and Fr.

Scaling of temperature and NDVI not only facilitates comparison between images and scatterplots, but it greatly reduces measurement error, eliminating the need for a detailed knowledge of plant, soil or atmospheric conditions. We can also show that scaling temperature greatly reduces the atmospheric correction to the thermal radiances, just as scaling NDVI virtually eliminates the need to correct N* for atmospheric attenuation (Figure 21).

To the extent that the uncorrected and corrected NDVI values are linearly related, the atmospheric correction is eliminated from N* in scaling. Indeed, we find this to be the case (Carlson and Ripley, in prep.). The result of scaling is that virtually identical values of Mo and Fr are obtained for corrected and uncorrected values of NDVI. Errors in Mo produced by not scaling the surface radiant temperature occur because the uncorrected temperatures are not linearly related to the corrected surface temperature. In split window models, such as that of Price (1984), the atmospheric corrections depend on differences in apparent temperatures between channel 4 and channel 5 of AVHRR, and so are not necessarily linearly related to the temperature of either channel.

Consider first a scatterplot for one of the Chester images (Figure 22). Using the Price split window method we first corrected every surface temperature and then found a linear regression between the temperature corrected with MODTRAN for channel 4 of AVHRR and the apparent (uncorrected) temperature, as measured by the satellite. This established a unique correction for each value of surface temperature although the slope and intercept of the regression are based on the split window results. RMS differences between this straight line fit to the split window temperatures and the temperatures given by the split window algorithm for each pixel provide an estimate of the 'typical error' one might encounter by collapsing the split window algorithm to a simple linear regression. (The word 'error' here is simply a measure of the scatter from a straight line, as there is some question as to whether this scatter represents noise or real varia-

tions.) The RMS error in the (non-dimensional) normalized temperature (T*) for the test case (Figure 22) was ±0.08. This value constitutes a relatively small fraction of the full range in T*, which varies from zero to one, respectively, between air temperature and the radiometric temperature of dry, bare soil.

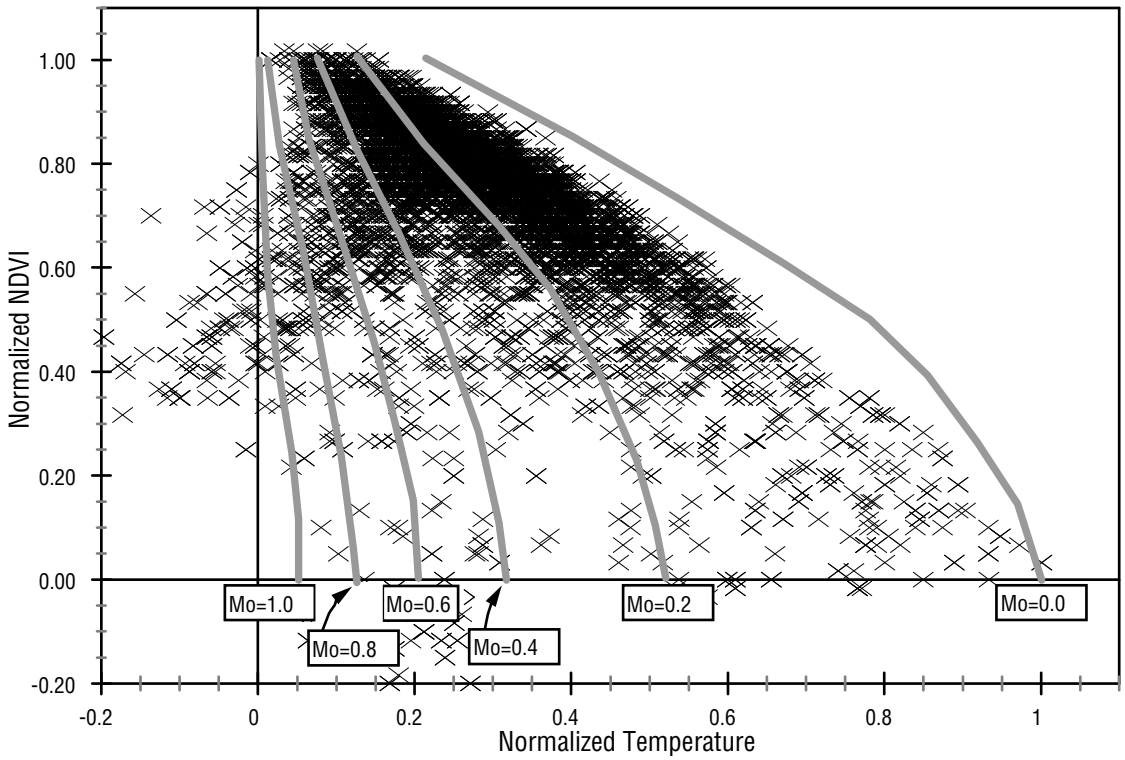

Figure 22. Scatterplot for the NOAA/AVHH image over Chester Co., 25 July, 1985. Normalized surface radiant temperature (T*) versus scaled NDVI (N*). The sloping vertical lines are isopleths of moisture availability (Mo)

To obtain isopleths of Mo, a polynomial relationship between Mo, N*, and T* is determined by making a range of simulations with our SVAT model (Gillies and Carlson, 1995). From this output, Mo is expressed as a function of the two scaled variables; isopleths of Mo are shown in Figure 22.

From this we also compute the following expression:

$$\Delta M_0(N^*,T^*) \approx \partial M_0 / \partial T^*[\Delta T^*]$$

where the partial derivative is determined by the functional form of Mo lines obtained from the simulations (the sloping lines in Figure 22) and the term in brackets on the right hand side is the RMS error referred to above. Note that this is really an estimate of the expected error in Mo based on a single case and may not precisely represent the error one would obtain in not using the split window on any other case. Further analyses of the remaining 13 AVHRR images for the Chester Co. area is being undertaken.

The implications of Figures 22 and 23 are similar to those for Figure 21 in the case of N*. The residual error in not making atmospheric corrections to surface radiant temperature is generally less than 0.2 in Mo (20% of the full range) except for the ranges of large Mo (above 0.5–0.8) and large Fr (above 80%). Inasmuch as most of the points in this scatterplot lie outside this range (except for densely vegetated areas) in this test case (Figure 22), the percentage of pixels suffering a significant degradation in Mo due to neglect of an atmospheric correction is quite small. Two important implications can be drawn from this result: First, scaling is a powerful tool which may permit the use of uncorrected surface radiant temperatures, at least in an operational mode, to determine Mo and Fr from satellite data. This shortcut would significantly reduce the work required for data reduction. Second, use of a split window algorithm may not yield significant improvement over a linear least squares relationship between corrected and measured surface radiant temperature.

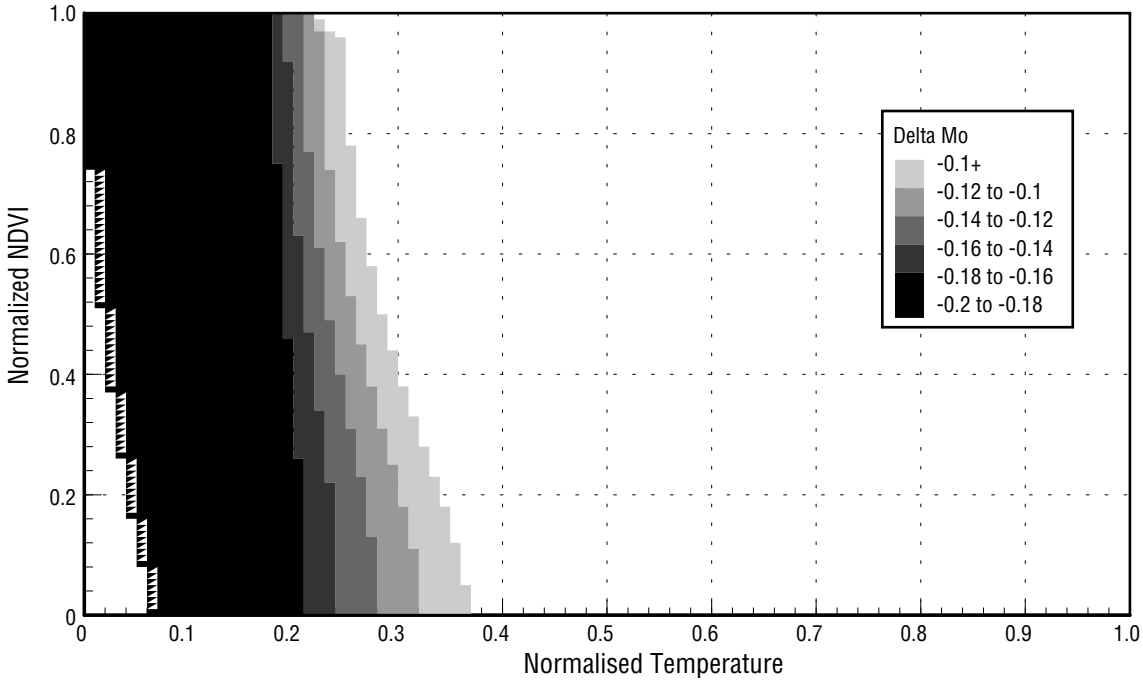

Figure 23. Normalized surface radiant temperature (T*) versus scaled NDVI (N*). The shaded area corresponds to the domain of the shaded region (the triangle) in figure 22 and the dark shaded area to the part of the triangle where the RMS 'error' in Mo (the RMS difference between Mo obtained from surface radiant temperatures corrected with a split window algorithm and those from uncorrected temperatures) exceeds 20% of the value of Mo. (Based on the NOAA/AVHH image over Chester Co., 25 July, 1985.)

It is our intention to make the triangle method useful to the scientific community. As a first step we are creating a web site (http://www.essc.psu.edu/~tnc), from which one can access instructions on how to apply the triangle method and how to access and execute the algorithms from which Mo/Fr isopleths and scatterplots can be generated.

Summary and Future Work

We intend to extend our State College analyses in new directions, tying the land use changes within the context of the triangle to socioeconomic changes in the region and to possible local climate and surface hydrology changes produced by urbanization. Ideally, we would like to produce a description of land use changes and urban development for Chester Co. in terms of changes

in the climate parameters, Mo and Fr, and in the land use index developed by Owen and Carlson (1996). For Costa Rica, we will relate the changes in land surface parameters, Mo and Fr, to the so-called 'life zone' which represent areas of more or less uniform ecology. Although most of the rampant deforestation in Costa Rica has been checked during the past 5 years, our image library extends back to the 1970s when deforestation was among the highest in the world.

Preliminary results for Chester Co. show that urbanization can be detected throughout the county during the period 1987–1996, with an increase in percent of area developed from about 11 in 1987 to about 19% in 1996. Urbanization is exploding throughout the countryside and expanding rapidly from roads and highways.

Chester Co. analyses should be completed early in 1997; all Costa Rican scenes will be completed and scatterplots prepared by mid 1997. Although the Chester Co. work should be completed by the end of summer 1997, we are hopeful that this research will continue in some form beyond 1997. In anticipation that the Chester Co. results will prove to be very interesting, we have requested continued satellite coverage of both Chester Co. and Costa Rica from the ASTER project, beginning in 1998. Coverage requests, recently submitted to the ASTER project at NASA, are modest; they amount to two or three scenes every summer for Chester Co. and about the same number of scenes during the dry season (Dec–Feb) for Costa Rica. ASTER's 30 m surface resolution will allow it to replace Landsat for image classification, but its several thermal IR channels will also permit the use of split window corrections schemes for surface radiant temperature, if indeed these corrections are required. This is currently possible only with AVHRR. Depending on the morning overpass time, ASTER may also replace AVHRR, whose overpass times are close to that of maximum surface temperature.

It is our hope that the triangle method can be simplified and streamlined such that it will lend itself to a routine applications. In so doing, it may be possible to use the fractional vegetation cover and moisture availability not only as key land use parameters in climate models but as unique indices of land use change which provide added descriptors of urbanization and deforestation beyond the conventional parameters already being employed by county planning boards.

Finally, we will be presenting a poster at an international meeting on remote sensing in France, (Physical Measurements & Signatures in Remote Sensing), to be held in Courchevel between 7 and 11 April, 1997. The subject of our poster is urbanization and deforestation in Chester Co. and Costa Rica, as viewed using the triangle method.

Water Quality Model

(L. Kump, P. Richards—PSU)

This year has been a transitional time for the water quality modeling effort. We have completed our analysis of the controls on the riverine chemistry of the major (weathering derived) elements, and have developed empirical relationships that can be used to predict stream chemical responses from the output of the Terrestrial Hydrology Model. These relationships are presented in the Ph.D. dissertation of Paul Richards (Richards, 1997) as well as in a papers in press in Hydrological Processes (Richards and Kump, 1997). In addition, we have assessed the effects that temperature has on chemical yields from small watersheds (Richards et al., submitted). Now we have turned our efforts to an analysis of nutrient distributions in the Susquehanna River Basin, and together with the Land Analysis Laboratory at Penn State, are compiling nutrient data for hundreds of small watersheds in the basin. These data are being stored in the SRBEX database, and will be used in the next year to develop empirical relationships between stream water quality and the factors that are thought to control it (and can be determined remotely), including land

cover and use, bedrock lithology, and climate (temperature and rainfall/runoff). As part of the collaborative effort with the Land Analysis Laboratory we have developed the following coverages for the Susquehanna River Basin:

- All streams for Pennsylvania, Maryland, and Virginia
- All watershed divides for Virginia, Pennsylvania, Maryland, and West Virginia
- Point coverage for every USGS gauge station in Pennsylvania
- EMAP 25m resolution for Pennsylvania
- Nutrient data for ~50 stations (out of a total of ~600)
- Most discharge data for Pennsylvania

These data will be statistically analyzed, as we have previously outlined for the major dissolved components (Richards and Kump, 1997). From this analysis we will develop the empirical model to be appended to the THM. This will allow us to assess the impact of predicted land-use changes and modelled climate changes in the next century on nutrient loadings on the Chesapeake Bay, as well as the response of the Susquehanna River's water quality on shorter (storm response, seasonal) timescales.

Spin-Off Human Dimensions Research On The Susquehanna River Basin

If long-range projections of the Susquehanna River Basin's hydrology are to be accurate, the human dimensions of regional climate-hydrology interactions must be incorporated into the SRBEX research design. However, because it is necessary to focus present NASA EOS funds on understanding the physical dimensions of the research, the vital human dimensions must be supported by outside funds. Four human dimensions projects are underway that are the direct result of the initial SRBEX impetus (details listed below). Each project involves at least two NASA EOS investigators and is either wholly or significantly focused on the hydroclimatology of the Susquehanna River Basin.

> EPA Office of Policy, Planning, and Evaluation: Global Climate Change Impacts on Water Resources And Ecosystems. (10/1/95–9/30/00; Cooperative Agreement); PI: A. Fisher;
>
> Co-PI: J. Shortle; with 8 Investigators, including 2 NASA EOS investigators. EPA Office of Research and Development: Regional Hydrologic Vulnerability and Adaptation to Climate: An Integrated Assessment of the Susquehanna River Basin. (11/1/95–10/31/98); PI: B. Yarnal; Co-PIs: R. Crane, J. Lynch and A. Fisher.
>
> NSF Global Change Program: Methods for Integrated Regional Assessment (06/15/96–06/14/2001); PI: C.G. Knight; with 10 Co-PIs, including three NASA EOS investigators.
>
> EPA Office of Research and Development: An Integrated Approach for Effective Representation and Analysis of Space-Time Environmental Data (9/01/96 to 8/31/99); PI: D. Peuquet; Co-PI:

GIS and Data Management System

(R.W. White, D.A. Miller, P.J. Kolb—PSU)

The GIS and data management system used to support our EOS investigation continued to grow during 1996. The aim of the system is to provide easy access to data and documentation for a wide range of spatial and tabular information in support of our research objectives. We continued to enhance our delivery of this information to not only our research team, but to researchers around the world through the World Wide Web. In particular, we have begun to place on the ESSC WWW server "customized" spatial data sets of land surface properties for use in a number of NASA and NOAA-sponsored projects including the Southern Great Plains '97 Experiment (a new EOS Interdisciplinary Science Team) and the NOAA-sponsored Global Energy and Water Cycle Experiment (GEWEX) Continental-Scale International Project (GCIP).

We have also remained actively involved with the EOS Data and Information System (EOSDIS), the EOS Calibration and Validation effort, and the EOS ASTER Instrument team. Richard White participated in a EOSDIS user interface prototypes workshop held at the Eros Data Center in Sioux Falls, SD. Doug Miller participated in a series of workshops covering calibration and validation issues for the EOS AM platform instruments. We were also involved in data format and projection discussions for the ASTER Level 1 data products.

References

Balling, R.C. and J.R. Christy, 1996: Analysis of satellite-based estimates of tropospheric diurnal temperature range. J. Geophys. Res., 101, 12827–12832.

Barron, E.J., G. Jenkins, M. Lakhatakia, D. Johnson, A. Miller, B. Yarnal, B. Frakes, D. White, and D. Miller, 1996: Results of coupled GCM-Mesoscale climate experiments. Workshop on High Resolution Modeling, Wengen, Switzerland, September 1996.

Barron, E.J. and G. Jenkins, (In Preparation): An AMIP (1979–1988) coupled GCM-Mesoscale Model Experiment.

Barron, E. J. and G. Jenkins, (In Preparation): Comparison of coupled GCM-Mesoscale Model experiments: Assessment of the importance of sea surface temperatures and carbon dioxide.

Barron, E. J. and G.S. Jenkins, 1995: ECMWF and GENESIS GCM coupled regional climate simulations for the summer of 1988. EOS Trans. AGU 76 (46). Fall Meeting Suppl. F92.

Barros, A.P., R. Bindlish, and A. Rogowski, (In Preparation): On the Use of a Hydrologically Oriented Classification of Soils.

Barros, A.P., and Evans, J., 1997: Designing for Climate Variability. J. of Prof. Issues Eng. Ed. and Prac., 123, 1-4.

Barros, A.P., 1995: Adaptive multilevel modeling of land-atmosphere interactions. J. Climate, 8, 2144-2160.

Barros, A.P., R. Bindlish, and G. Jenkins, 1996: The role of the coupled land-atmosphere-ocean system on the occurrence of extreme floods and droughts. Preprint Vol. Second Int. Con. on the Global Energy and Water Cycle, June 17–22, 1996 Washington, World Climate Research Program, Global Energy and Water Cycle Experiment. DC. p.21.

Bechtold, P., S.K. Krueger, W.S. Lewellen, E. Van Meijgaard, C.-H. Moemg, D.A. Randall, A Van Ulden, and S. Wang, 1996: Modeling a stratocumulus-topped PBL: Intercomparison among different one-dimensional codes and with large eddy simulation. Bull. Amer. Meteor. Soc., 77, 2033–2042.

Bindlish, R. and A.P. Barros, 1996a: Aggregation of digital terrain data using a modified fractal interpolation scheme. Comp. Geosci. 22, 907–917.

Bindlish, R. and A.P. Barros, (In Preparation): Analysis of the Space-Time Properties of Remotely-Sensed Soil Moisture.

Bindlish, A.P., and Barros, R., 1996b (Under revision): Quantitative Description of the Space-Time properties of Climate Variables: An Intercomparison of ISCCP, GENESIS and CCM2 Cloud Fields. J. Climate.

Bindlish, R., and A.P. Barros, 1997: On the characterization of hydrologically relevant soil properties using remotely-sensed data. Preprints of the 13th Con. on Hydro. Long Beach, CA. February 2–7, 1997. American Meteorological Society, Boston, MA.

Capehart, W.J., and T.N. Carlson, 1994: Estimating near-surface soil moisture availability using a meteorologically driven soil water profile model. J. Hydro., 160, 1–20.

Carlson, T. N. and T. W. Owen, 1996: Monitoring urbanization and urban climate by satellite. Proc. Symp.on Monitoring Urbanization and Urban Climate by Satellite, Human Interactions with the Environment, Pecora 13 Symposium, Sioux Falls, SD, August, 20–22, 1996.

Carlson, T. N. and D. A. J. Ripley, (In Preparation): On the Relationship between NDVI, Fractional Vegetation Cover and Leaf Area Index.

Carlson, T.N., D.A.J. Ripley, W.J. Capehart, and D.A. Miller, 1996: Decoupling of surface soil water content:A problem in remote sensing. EOS Trans. AGU 77 (17) Spring Meeting Suppl. S123.

Choudhury, B. J., N. U. Ahmed, S. B. Idso, R. J. Reginato and C. S.T. Daughtry, 1994: Relations between evaporation coefficients and vegetation indices studied by model simulations. Remote Sens. Environ., 50, 1–17.

Christy, J.R., 1995: Temperature above the surface layer. Climatic Change, 31, 455–474.

Christy, J.R. and R.T. McNider, 1994: Satellite greenhouse signal. Nature, 367, 325.

Congalton, R. G., 1991: A review of assessing the accuracy of classifications of remotely sensed data, Rem. Sens. Environ., 37, 35–46.

Duffy, C.J. 1996. Stochastic resonance and nonlinear groundwater reservoirs: a case for amplification of low-frequency climate signals. EOS Trans. AGU 77 (46) Fall Meeting Suppl. F40.

Eliasziw, M., 1991: Application of the McNemar test to non-independent matched pair data. Statistics in Medicine, 10 (12), 1981.

Frakes, B. and Yarnal, B., 1996a (Submitted): A synoptic climatology of river-basin response to storm events (submitted to Annals of the Association of American Geographers).

Frakes, B. and Yarnal, B., 1996b (Submitted): A synoptic climatology of strong river-basin discharge (submitted to Physical Geography).

Frakes, B. and Yarnal, B., 1996c (Submitted): A combined manual and automated technique for synoptic classification (submitted to International Journal of Climatology).

Gillies, R .R. and T. N. Carlson, 1995: Thermal remote sensing of surface soil water content with partial vegetation cover for incorporation into climate models, J. Appl. Meteor. 34, 745–756.

Hewitson, B. C. and R.G. Crane, 1992a: Regional scale climate prediction from the GISS GCM. Global and Planetary Change, 97, 249–267.

Hewitson, B. C. and Crane, R. G. 1992b: Large-scale atmospheric controls on local precipitation in tropical Mexico. Geophys. Res. Lett., 19(18), 1835–1838.

Jenkins, G.S. and E.J. Barron, 1997a (In Press): General circulation model and coupled regional climate model simulations over the eastern United States: Genesis and RegCM2 simulations. Global and Planetary Change

Jenkins, G.S. and E.J. Barron, 1997b: Decade-long coupled GCM/Regional Climate Model Simulations over the United States AMS Meeting, Long Beach, CA 1997.

Jenkins, G.S. and E.J. Barron, (In Preparation): A sensitivity study of a Regional Climate model experiments during the summer of 1988 using boundary conditions from ECMWF analyses and the GENESIS GCM. I: Large scale circulation.

Karl, T. R., W.-C. Wang, M.E. Schlesinger, R.W. Knight and D. Portman, 1990: A method of relating general circulation model simulated climate to the observed local climate. Part I: Seasonal statistics. J. Climate, 3, 1053–1079.

Kneizys, F. X., E. P. Shettle, L. W. Abreu, J. H. Chetwynd, G. P. Anderson, W. O. Gallery, J. E. Selby, S. A. Clough, 1988: Users Guide to Lowtran-7. Air Force Geophysics Laboratory Research Paper 401010, Project 7670. 34 pp.

Lakhtakia, M.N. (In Preparation): On improving near-real-time precipitation analyses.

Lakhtakia, M.N., D.A. Miller, R.A. White, and C.B. Smith, 1996: GIS as an integrative tool in climate and hydrology modeling. In: GIS and Environmental Modeling (M.F. Goodchild, L.T. Steyaert, B.O. Parks, C. Johnston, D. Maidment, M. Crane, & S. Glendinning, eds.). GIS World, Inc., Fort Collins, CO. p.309–312.

Lakhtakia, M.N., C.B. Smith, T.N. Carlson, W.J. Capehart, and A.M. Lario, 1994a: Initialization of soil-water content for regional-Scale Atmospheric Prediction Models. EOS Trans. AGU 75(16) Spring Meeting Suppl. 97.

Lakhtakia, M.N., A.M. Lario, and T.N. Carlson, 1994b: Initialization of soil-water content for real-time simulations with the Penn State/NCAR mesoscale model. Preprints of the Tenth Con. on Num. Weather Predict. Portland, Oregon July 18–22, 1995. American Meterological Society, Boston, MA. p.428–429.

Lakhtakia, M.N., and T.T. Warner, 1994: A comparison of simple and complex treatments of surface hydrology and thermodynamics suitable for mesoscale atmospheric models. Mon. Wea. Rev., 122, 880–896.

Lapenta, W.L., M. Lakhtakia, F.R. Robertson, R.T. McNider, A.Song, and J. Luvall, 1997: Application of remotely sensed data to land surface/atmosphere coupled modeling Issues. Preprints of the 8th Symp. on Global Change Studies, Long Beach CA, February 2-7, 1997. American Meteorological Society, Boston, MA.

Loveland, T.R., J.W. Merchant, D.O. Ohlen, and J.F. Brown, 1991: Development of a land-cover characteristics database for the conterminous U. S. Photogrammetric Engineering & Remote Sensing, 57, 1453–1463.

Miller, D.A. and R,A, White, 1996: A 1 Km Continental United States Multi-Layer Soil Characteristics Data Set for Climate and Hydrology Modeling. Preprint Vol. Second Int. Con. on the Global Energy and Water Cycle, Washington DC. World Climate Research Program, Global Energy and Water Cycle Experiment. p. 219.

Miller, D.A. and R.A. White, (In Preparation): A Conterminous United States Multi-Layer Soil Characteristics Data Set for Regional Climates and Hydrology Modelling.

Miller, D.A. and S.E. Hollinger, 1997: Planning in-site soil moisture observations for climate and hydrology studies. Preprints of the 13th Con. on Hydro. Long Beach, CA. February 2–7, 1997. American Meteorological Society, Boston, MA.

Owen, T.W., 1995: An approach towards quantifying the climate effect of urbanization using satellite remote sensed land cover parameters. Unpublished MS thesis, Department of Meteorology, The Pennsylvania State University, university Park, PA.

Owen, T. W., T. N. Carlson and R. R. Gillies, (Submitted): As assessment of satellite remotely sensed land cover parameters in quantitatively describing the climate effect of urbanization. Int. J. Remote Sensing.

Parker, D.E., H. Wilson, P.D. Jones, J.R. Christy and C.K. Folland, 1996: The impact of Mount Pinatubo on world-wide temperatures. Int. J. Climatology, 16, 487–497.

Peterson, W.H., G.S. Jenkins, E.J. Barron, 1995: Evaluation of GENESIS and coupled GENESIS/RegCM2 simulations during the 1979–1988 period. EOS Trans. AGU 76 (46). Fall Meeting Suppl. F111.

Price, J. C., 1984: Land surface temperature measurements from the split window channels of NOAA-7/AVHRR. J. Geophys. Res., 100, 81–92.

Raghavan, R., S. Goodman, P. Meyer, and D. Buechler, (In preparation): A convective-stratiform rainfall classifier for composite radar reflectivity maps. J. Appl. Meteor.

Richards, P.L., Brantley, S., and Kump, L.R., (Submitted). Soil porewater distributions and the temperature dependence of weathering in the field. Geochimica et Cosmochimica Acta.

Richards, P.L. and Kump, L.R., 1997: Application of the GIS approach to watershed mass-balance studies. Hydrological Processes (In Press).

Richards, P.L., 1997. The hydrology and geochemistry of weathering. Unpublished Ph.D. Dissertation, Department of Geosciences. The Pennsylvania State University, University Park, PA.

Robertson, F. R., D.E. Fitzjarrald, and W.D. Braswell, 1997 (Submitted): Interannual variability in TOA LWCS fluxes: An intercomparison of three satellite estimates. J. Geophys. Res.

Robertson, F. R., W.D. Braswell, and D.E. Fitzjarrald, 1997 (Submitted): The effect of interannual variability in water vapor and lapse rate on tropical energy balance. J. Geophys. Res.

Robertson, F.R., W.D. Braswell, and D. Fitzjarrald, 1996: Anomalies In radiation, heat and water budgets as diagnosed from pre-Eos data sets: Insights on tropical climate sensitivity. Preprint Vol. Second Int. Con. on the Global Energy and Water Cycle, Washington DC. World Climate Research Program, Global Energy and Water Cycle Experiment. p.412.

Robertson, F.R., W.D. Braswell, and D. Fitzjarrald, 1996: Water vapor feedback deduced from interannual variability in ERBE fluxes. Workshop on Climate Sensitivity. April 21-22, 1996. MIT. Cambridge, MA.

Shun, T.-Y. and C.J. Duffy, 1996: Application of multichannel single spectrum analysis: Space-time construction for monthly runoff, precipitation and temperature fields in the Wasatch Range, Utah. EOS Trans. AGU 77 (17) Spring Meeting Suppl. S122.

Smith C.B., M.N. Lakhtakia, W.J. Capehart, and T.N. Carlson, 1994: Initialization of soil-water content in regional-scale atmospheric prediction models. Bull. Amer. Meteor. Soc., 74, 585–593.

Spencer, R.W., J.R. Christy and N.C. Grody, 1996: Examination of global atmospheric temperature monitoring with satellite microwave measurements. Climatic Change, 33, 477–489.

Tarboton, D.G. and C.H. Luce, 1996: Utah energy balance snow accumulation and melt model (UUB): computer model and technical description and users guide. Utah Water Research Laboratory, Utah State University, Logan Utah, 60-p.

Tarboton, D.G., T.G. Chowdhury, T.H. Jackson, 1995: A spatially distributed energy balance snow model. Biogeochemistry of Seasonally Snow-Covered Catchments (Proceedings of a Boulder Symposium, July 1995). IAS Publ No. 228 141–155.

Tin-Seong, K. A. M., 1995: Integrating GIS and remote sensing techniques for urban land cover and land use analysis. Geocarto. International, 10, 39–48.

Thompson, S. L. and D. Pollard, (Submitted): Greenland and Antarctic mass balances for present and doubled CO_2 from the GENESIS version 2 global climate model. J. Climate

Yarnal, B. and Frakes, B.J., 1997a: Using synoptic climatology to define representative discharge events. International Journal of Climatology 17, 1–18.

Yarnal, B. and Frakes, B. 1997b: A Synoptic Climatological Atlas of the Northeast United States. Northeast Regional Climate Center, Cornell University, Ithaca, NY

Wang, S., 1996a: A prognostic approach of parameterizing marine boundary-layer clouds. EOS Trans. AGU 77 (46), Fall Meeting Suppl., F229.

Wang, S., 1996b: Defining marine boundary-layer clouds with a prognostic scheme. Mon. Wea. Rev., 124, 1617–1833.

White, R.A. and D.A. Miller, (Submitted): Processing soil survey data with Perl. Comp. Geosci.

Wigley, T. M. L., P.D. Jones, K.R. Briffa, and G. Smith, 1990: Obtaining sub-grid-scale information from coarse-resolution general circulation model output. J. Geophys. Res., 95, 1943–1953.

Willmott, C. J., M.R. Clinton, and W.D. Philpot, 1985: Small-scale climate maps: A sensitivity analysis of some common assumptions associated with grid-point interpolation and contouring. Amer. Cart., 12, 5–16

1995–1996 EOS Contributions

Balling, R.C. and J.R. Christy, 1996: Analysis of satellite-based estimates of tropospheric diurnal temperature range. J. Geophys. Res., 101, 12827–12832.

Barron, E.J., G. Jenkins, M. Lakhatakia, D. Johnson, A. Miller, B. Yarnal, B. Frakes, D. White, and D. Miller, 1996: Results of coupled GCM-Mesoscale climate experiments. Workshop on High Resolution Modeling, Wengen, Switzerland, September 1996.

Barron, E.J. and G. Jenkins, (In Preparation): An AMIP (1979–1988) coupled GCM-Mesoscale Model Experiment.

Barron, E. J. and G. Jenkins, (In Preparation): Comparison of coupled GCM-Mesoscale Model experiments: Assessment of the importance of sea surface temperatures and carbon dioxide.

Barros, A.P., R. Bindlish, and A. Rogowski, (In Preparation): On the Use of a Hydrologically Oriented Classification of Soils.

Barros, A.P., and Evans, J., 1997: Designing for Climate Variability. J. of Prof. Issues Eng. Ed. and Prac., 123, 1-4.

Barros, A.P., 1995: Adaptive multilevel modeling of land-atmosphere interactions. J. Climate, 8, 2144-2160.

Barros, A.P., R. Bindlish, and G. Jenkins, 1996: The role of the coupled land-atmosphere-ocean system on the occurrence of extreme floods and droughts. Preprint Vol. Second Int. Con. on the Global Energy and Water Cycle, June 17–22, 1996 Washington, World Climate Research Program, Global Energy and Water Cycle Experiment. DC. p.21.

Bechtold, P., S.K. Krueger, W.S. Lewellen, E. Van Meijgaard, C.-H. Moemg, D.A. Randall, A Van Ulden, and S. Wang, 1996: Modeling a stratocumulus-topped PBL: Intercomparison among different one-dimensional codes and with large eddy simulation. Bull. Amer. Meteor. Soc., 77, 2033–2042.

Bindlish, R. and A.P. Barros, 1996a: Aggregation of digital terrain data using a modified fractal interpolation scheme. Comp. Geosci. 22, 907–917.

Bindlish, R. and A.P. Barros, (In Preparation): Analysis of the Space-Time Properties of Remotely-Sensed Soil Moisture.

Bindlish, A.P., and Barros, R., 1996b (Under revision): Quantitative Description of the Space-Time properties of Climate Variables: An Intercomparison of ISCCP, GENESIS and CCM2 Cloud Fields. J. Climate.

Bindlish, R., and A.P. Barros, 1997: On the characterization of hydrologically relevant soil properties using remotely-sensed data. Preprints of the 13th Con. on Hydro. Long Beach, CA. February 2–7, 1997. American Meteorological Society, Boston, MA.

Carlson, T. N. and T. W. Owen, 1996: Monitoring urbanization and urban climate by satellite. Proc. Symp.on Monitoring Urbanization and Urban Climate by Satellite, Human Interactions with the Environment, Pecora 13 Symposium, Sioux Falls, SD, August, 20–22, 1996.

Carlson, T. N. and D. A. J. Ripley, (In Preparation): On the Relationship between NDVI, Fractional Vegetation Cover and Leaf Area Index.

Carlson, T.N., D.A.J. Ripley, W.J. Capehart, and D.A. Miller, 1996: Decoupling of surface soil water content:A problem in remote sensing. EOS Trans. AGU 77 (17) Spring Meeting Suppl. S123.

Christy, J.R., 1995:Temperature above the surface layer. Climatic Change, 31, 455–474.

Duffy, C.J. 1996. Stochastic resonance and nonlinear groundwater reservoirs: a case for amplification of low-frequency climate signals. EOS Trans. AGU 77 (46) Fall Meeting Suppl. F40.

Frakes, B. and Yarnal, B., 1996a (Submitted): A synoptic climatology of river-basin response to storm events (submitted to Annals of the Association of American Geographers).

Frakes, B. and Yarnal, B., 1996b (Submitted):A synoptic climatology of strong river-basin discharge (submitted to Physical Geography).

Frakes, B. and Yarnal, B., 1996c (Submitted): A combined manual and automated technique for synoptic classification (submitted to International Journal of Climatology).

Gillies, R .R. and T. N. Carlson, 1995:Thermal remote sensing of surface soil water content with partial vegetation cover for incorporation into climate models, J. Appl. Meteor. 34, 745–756.

Jenkins, G.S. and E.J. Barron, 1997a (In Press): General circulation model and coupled regional climate model simulations over the eastern United States: Genesis and RegCM2 simulations. Global and Planetary Change

Jenkins, G.S. and E.J. Barron, 1997b: Decade-long coupled GCM/Regional Climate Model Simulations over the United States AMS Meeting, Long Beach, CA 1997.

Jenkins, G.S. and E.J. Barron, (In Preparation): A sensitivity study of a Regional Climate model experiments during the summer of 1988 using boundary conditions from ECMWF analyses and the GENESIS GCM. I: Large scale circulation.

Lakhtakia, M.N. (In Preparation): On improving near-real-time precipitation analyses.

Lakhtakia, M.N., D.A. Miller, R.A. White, and C.B. Smith, 1996: GIS as an integrative tool in climate and hydrology modeling. In: GIS and Environmental Modeling (M.F. Goodchild, L.T. Steyaert, B.O. Parks, C. Johnston, D. Maidment, M. Crane, & S. Glendinning, eds.). GIS World, Inc., Fort Collins, CO. p.309–312.

Lapenta, W.L., M. Lakhtakia, F.R. Robertson, R.T. McNider, A. Song, and J. Luvall, 1997: Application of remotely sensed data to land surface/atmosphere coupled modeling Issues. Preprints of the 8th Symp. on Global Change Studies, Long Beach CA, February 2-7, 1997. American Meteorological Society, Boston, MA.

Miller, D.A. and R,A, White, 1996: A 1 Km Continental United States Multi-Layer Soil Characteristics Data Set for Climate and Hydrology Modeling. Preprint Vol. Second Int. Con. on the Global Energy and Water Cycle, Washington DC. World Climate Research Program, Global Energy and Water Cycle Experiment. p. 219.

Miller, D.A. and R.A. White, (In Preparation): A Conterminous United States Multi-Layer Soil Characteristics Data Set for Regional Climates and Hydrology Modelling.

Miller, D.A. and S.E. Hollinger, 1997: Planning in-site soil moisture observations for climate and hydrology studies. Preprints of the 13th Con. on Hydro. Long Beach, CA. February 2–7, 1997. American Meteorological Society, Boston, MA.

Owen, T.W., 1995: An approach towards quantifying the climate effect of urbanization using satellite remote sensed land cover parameters. Unpublished MS thesis, Department of Meteorology, The Pennsylvania State University, university Park, PA.

Owen, T. W., T. N. Carlson and R. R. Gillies, (Submitted): As assessment of satellite remotely sensed land cover parameters in quantitatively describing the climate effect of urbanization. Int. J. Remote Sensing.

Parker, D.E., H. Wilson, P.D. Jones, J.R. Christy and C.K. Folland, 1996: The impact of Mount Pinatubo on world-wide temperatures. Int. J. Climatology, 16, 487–497.

Peterson, W.H., G.S. Jenkins, E.J. Barron, 1995: Evaluation of GENESIS and coupled GENESIS/RegCM2 simulations during the 1979–1988 period. EOS Trans. AGU 76 (46). Fall Meeting Suppl. F111.

Raghavan, R., S. Goodman, P. Meyer, and D. Buechler, (In preparation): A convective-stratiform rainfall classifier for composite radar reflectivity maps. J. Appl. Meteor.

Richards, P.L., Brantley, S., and Kump, L.R., (Submitted). Soil porewater distributions and the temperature dependence of weathering in the field. Geochimica et Cosmochimica Acta.

Richards, P.L. and Kump, L.R., 1997: Application of the GIS approach to watershed mass-balance studies. Hydrological Processes (In Press).

Richards, P.L., 1997. The hydrology and geochemistry of weathering. Unpublished Ph.D. Dissertation, Department of Geosciences. The Pennsylvania State University, University Park, PA.

Robertson, F. R., D.E. Fitzjarrald, and W.D. Braswell, 1997 (Submitted): Interannual variability in TOA LWCS fluxes: An intercomparison of three satellite estimates. J. Geophys. Res.

Robertson, F. R., W.D. Braswell, and D.E. Fitzjarrald, 1997 (Submitted): The effect of interannual variability in water vapor and lapse rate on tropical energy balance. J. Geophys. Res.

Robertson, F.R., W.D. Braswell, and D.Fitzjarrald, 1996: Anomalies In radiation, heat and water budgets as diagnosed from pre-Eos data sets: Insights on tropical climate sensitivity. Preprint Vol. Second Int. Con. on the Global Energy and Water Cycle, Washington DC. World Climate Research Program, Global Energy and Water Cycle Experiment. p.412.

Robertson, F.R., W.D. Braswell, and D.Fitzjarrald, 1996: Water vapor feedback deduced from interannual variability in ERBE fluxes. Workshop on Climate Sensitivity. April 21-22, 1996. MIT. Cambridge, MA.

Shun, T.-Y. and C.J. Duffy, 1996: Application of multichannel single spectrum analysis: Space-time construction for monthly runoff, precipitation and temperature fields in the Wasatch Range, Utah. EOS Trans. AGU 77 (17) Spring Meeting Suppl. S122.

Spencer, R.W., J.R. Christy and N.C. Grody, 1996: Examination of global atmospheric temperature monitoring with satellite microwave measurements. Climatic Change, 33, 477–489.

Yarnal, B. and Frakes, B.J., 1997a: Using synoptic climatology to define representative discharge events. International Journal of Climatology 17, 1–18.

Yarnal, B. and Frakes, B. 1997b: A Synoptic Climatological Atlas of the Northeast United States. Northeast Regional Climate Center, Cornell University, Ithaca, NY

Wang, S., 1996a: A prognostic approach of parameterizing marine boundary-layer clouds. EOS Trans. AGU 77 (46), Fall Meeting Suppl., F229.

Wang, S., 1996b: Defining marine boundary-layer clouds with a prognostic scheme. Mon. Wea. Rev., 124, 1617–1833.

White, R.A. and D.A. Miller, (Submitted): Processing soil survey data with Perl. Comp. Geosci.